





## ORIGINAL RESEARCH ARTICLE

## Integrated Phytochemical Profiling (GC-MS/FTIR), Molecular Docking, and Bioevaluation of *Vernonia amygdalina* and *Psidium guajava* Against Multidrug-Resistant *Salmonella typhi*

Zaharaddeen Usman<sup>1</sup> , Fatima Mukhtar\*<sup>1</sup> , Baha'uddeen Salisu<sup>1</sup>  & Abdulbari Saleh Dandashire<sup>2</sup> <sup>1</sup>Department of Microbiology, Faculty of Natural and Applied Sciences, Umaru Musa Yar'adua University, Katsina, Nigeria<sup>2</sup>Department of Applied Geology, Faculty of Science, Abubakar Tafawa Balewa University, P.M.B. 0248, Bauchi, Nigeria

### ABSTRACT

Typhoid fever is caused by *Salmonella enterica* serovar *Typhi* (*S. Typhi*). It is a major public health challenge in resource-limited settings, especially when multidrug-resistant (MDR) strains of *S. Typhi* are encountered, as they generally complicate treatment. This research assessed the phytochemical qualities and bioactivities of *Vernonia amygdalina* (Bitter Leaf) and *Psidium guajava* (Guava) for their ability to inhibit the growth of MDR *S. Typhi*. The disk diffusion and broth dilution methods were used to test the antimicrobial activity of methanolic agar. *V. amygdalina* had a relatively higher activity with an inhibition zone (ZOI) of 11–14 mm, minimum inhibitory concentration (MIC) of 50 mg/mL and minimum bactericidal concentration (MBC) of 100 mg/mL compared to *P. guajava* with an inhibition zone (ZOI) of 10–13 mm, minimum inhibitory concentration (MIC) of 100 mg/mL and minimum bactericidal concentration (MBC) of 150 mg/mL. The joint use of *V. amygdalina* and *P. guajava* gave better results (ZOI: 14–18.5 mm; MIC/MBC: 50 mg/mL). Using chromatography, the major bioactive components were identified as thymol, limonene and oleic acid, which showed high binding affinity to *S. typhi*. In silico docking studies were used to evaluate targets of *S. typhi* virulence, including DNA gyrase and the SipD protein. Safety evaluations of the extracts at therapeutic doses in Wistar rats, using acute and subchronic toxicity tests, did not cause any lethality or severe adverse effects. Histopathological and biochemical studies showed mild hepatorenal effects at high doses, reversible. The results bolster the ancient use of these plants and indicate their potential as alternative or supplementary medicines for MDR typhoid fever. Future research should focus on clinical trials to further develop formulations and investigate mechanisms to realize their clinical applications.

### ARTICLE HISTORY

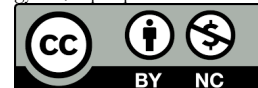
Received September 13, 2025

Accepted December 07, 2025

Published December 29, 2025

### KEYWORDS

Chromatography, DNA gyrase, SipD protein



© The Author(s). This is an Open Access article distributed under the terms of the Creative Commons Attribution 4.0 License [creativecommons.org](https://creativecommons.org/licenses/by-nc/4.0/)

### INTRODUCTION

Typhoid fever is a serious infectious disease with systemic manifestations caused by *Salmonella enterica* serovar *Typhi*, a gram-negative bacterium. The illness is characterized by high fever, abdominal pain, and other systemic complications. It's a disease that mainly affects humans, with no known animal reservoirs, and is a major public health concern in areas with poor sanitation and inadequate access to safe water (WHO, 2023).

*S. Typhi* is a bacterium that can move and has many virulence factors to cause disease. *Salmonella Typhi* evades the immune system because of its unique lipopolysaccharide (LPS) structure. The Vi capsular polysaccharide resists complement activation and phagocytosis. The bacterium can intrinsically invade the epithelial cells and macrophages of the small intestine after surviving the acidic conditions of the stomach and gaining

access to the bloodstream and lymphatic system (Al-Khafaji *et al.*, 2022).

Once in the bloodstream, *S. Typhi* can spread to various organs such as the liver, spleen, bone marrow and lymphatic tissue. The pathogen's affection of these organs causes systemic effects, such as high fever and abdominal pain, which should not be neglected. Typhoid fever can cause death as a result of GI bleeding, intestinal perforation, septic shock, etc due to which, if the antimicrobial treatment is not started in a timely and proper manner (WHO, 2023).

The main mode of transmission for *S. Typhi* is the faecal-oral route. Infected people's faeces contaminate food or water, which is how the bacterium usually spreads. The risk factors for typhoid fever transmission (WHO, 2023)

**Correspondence:** Fatima Mukhtar. Department of Microbiology, Faculty of Natural and Applied Sciences, Umaru Musa Yar'adua University, Katsina, Nigeria. ✉ [fatima.mukhtar@umyu.edu.ng](mailto:fatima.mukhtar@umyu.edu.ng)

**How to cite:** Usman, Z., Mukhtar, F., Salisu, B., & Saleh, A. D. (2025). Integrated Phytochemical Profiling (GC-MS/FTIR), Molecular Docking, and Bioevaluation of *Vernonia amygdalina* and *Psidium guajava* Against Multidrug-Resistant *Salmonella typhi*. *UMYU Scientifica*, 4(4), 88 – 111. <https://doi.org/10.56919/usci.2544.009>

include poor sanitation, inadequate wastewater treatment, and improper food handling. In areas where safe drinking water and sanitation are in short supply, *S. Typhi* is transmitted, leading to endemic outbreaks.

Most commonly, humans spread this virus to one another. Infected individuals shed *S. Typhi* when they pass the bacteria, which are excreted in their faeces and urine. Also, the non-sick who have the bacteria in their gallbladders help maintain the cycle of infection. These carriers can shed the pathogen into the environment years after infection without showing clinical symptoms. [Bhandari et al. \(2024\)](#) It would be challenging to contain outbreaks, as asymptomatic individuals can infect others without knowing they are infected ([Shaikh et al., 2023](#)).

Besides the faecal-oral route, one can get infected through contact with an infected person or contaminated surfaces. This is rare, however, and insufficient for water-borne transmission. Nonetheless, in congested, dirty areas, there is a high risk of direct transmission, especially when people do not maintain proper hygiene ([Zafar et al., 2024](#)).

The effectiveness of the plants used by a large number of people lacks scientific research and evidence-based validation. Molecular docking studies and bioscreening of these plants can provide strong scientific validation for their use in modern medicine. Moreover, ethnobotanical information on traditional medicine can assist in the discovery of new drugs by flagging plant types with potential therapeutic value ([Rigby, 2024](#)). This study aims to evaluate the antibacterial efficacy, phytochemical composition, mechanism of action, and safety of *Vernonia amygdalina* (Bitter Leaf) and *Psidium guajava* (Guava) for the treatment of typhoid fever, with a focus on their activity against multidrug-resistant (MDR) *Salmonella typhi* isolates.

## MATERIALS AND METHOD

### Study Area

This study was conducted in Katsina State, Northern Nigeria. It borders the Republic of Niger to the North, Kaduna to the South, Zamfara to the West and Kano and Jigawa to the East. Katsina State covers an area of 23,938 km<sup>2</sup>, equivalent to about 2.7% of Nigeria's total land area. The state is divided into 34 Local Government Areas ([Ahmed et al., 2025](#)).

### Collection of Bacterial Strains and Culture Conditions

A fifteen (15) clinical sample of *Salmonella enterica serovar Typhi* were obtained from the microbiology laboratory of Katsina General Hospital. These samples were collected between January and December 2024 from patients with confirmed typhoid fever. All samples were confirmed as *S. Typhi* in the microbiology laboratory at Umaru Musa Yar'adua University, Katsina. The procedure described by [Sankar et al. \(2025\)](#) was followed to generate Columbia agar enhanced with 5% sheep blood. Antibiotics were subsequently added to this agar to strengthen it and stop contamination. The agar was produced, frozen stocks of *S. Typhi* cultures were added, and the mixture was grown

in a microaerobic environment for two to three days at 37°C.

### Antibiotic Susceptibility Testing of *S. Typhi* Isolates to Screen for MDR Strain

To establish a baseline for antimicrobial resistance and provide a direct comparator for the plant extracts, fifteen (15) recent clinical samples of *Salmonella enterica serovar Typhi* were obtained from the microbiology laboratory of Katsina General Hospital.

The antibiotic susceptibility of these isolates was evaluated against three first-line antibiotics, each representing a distinct class: **Ciprofloxacin (Fluoroquinolone)**: Inhibits DNA gyrase and topoisomerase IV. **Ceftriaxone (Third-generation Cephalosporin)**: Inhibits cell wall synthesis. **Azithromycin (Macrolide)**: Inhibits protein synthesis by binding to the 50S ribosomal subunit. Testing was performed using the disc diffusion method on Mueller-Hinton agar, in accordance with the Clinical and Laboratory Standards Institute ([CLSI, 2023](#)) performance standards. Briefly, a 0.5 McFarland standard suspension of each *S. Typhi* isolate was swabbed onto Mueller-Hinton agar plates. Antibiotic discs with the following potencies were aseptically placed on the inoculated plates: Ciprofloxacin (5 µg), Ceftriaxone (30 µg), and Azithromycin (15 µg). The plates were incubated at 37°C for 16-24 hours. The diameters of the zones of inhibition (ZOI) were measured in millimeters and interpreted as Susceptible (S), Intermediate (I), or Resistant (R) based on CLSI breakpoint criteria.

### Collection of Plant Samples and Identification

Plant leaves, stems, and roots were gathered from the Umaru Musa Yar'adua University botanical gardens in Katsina, as well as from nearby traditional healers'. A trained botanist botanically identified these plants, and a special voucher specimen number was assigned to the university herbarium for future use and record-keeping ([Greene et al., 2023](#)). The newly harvested leaves, stems, and roots were air-dried in a shaded place for 10 to 15 days after being cleaned with distilled water and rinsed with tap water using the method described by [Krakowska-Sieprawska et al. \(2022\)](#). The dehydrated plant material was next ground into a fine powder, placed in opaque containers, and chilled until it was time to use.

### Preparation of Plants Extracts

The powder obtained from the plants underwent a sequential extraction process using deionized water, modified from the methodology described by [Verep et al. \(2023\)](#). Five (5) grams of the powdered plants were weighed and put in a thimble within a Soxhlet device. From there, they were extracted over 4 hours at 45°C using 50 mL of water after soaking overnight. The extracted mixture was collected in a conical flask, concentrated using a rotary evaporator at low temperature and reduced pressure, and frozen overnight. It was then kept refrigerated until needed for the assay.

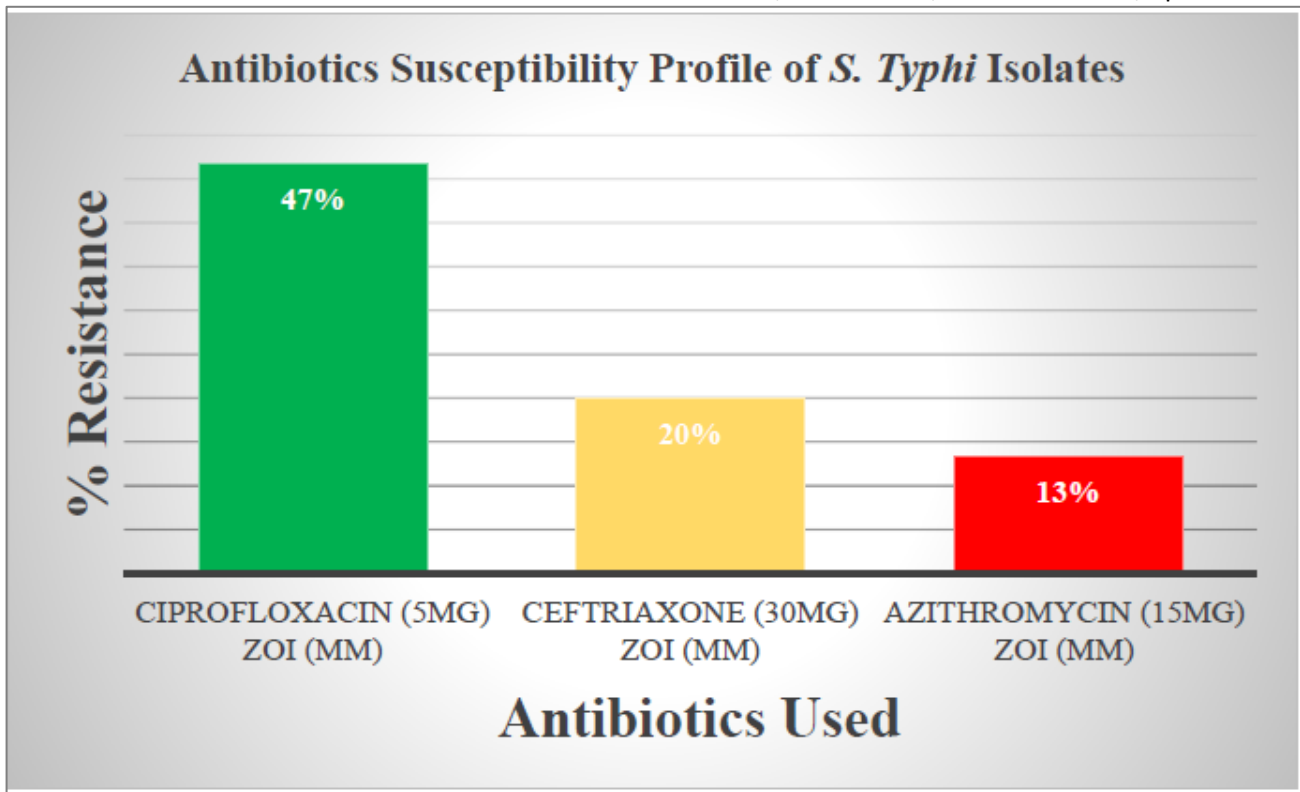


Figure 1: Antibiotic susceptibility profile of *S. Typhi* Isolate

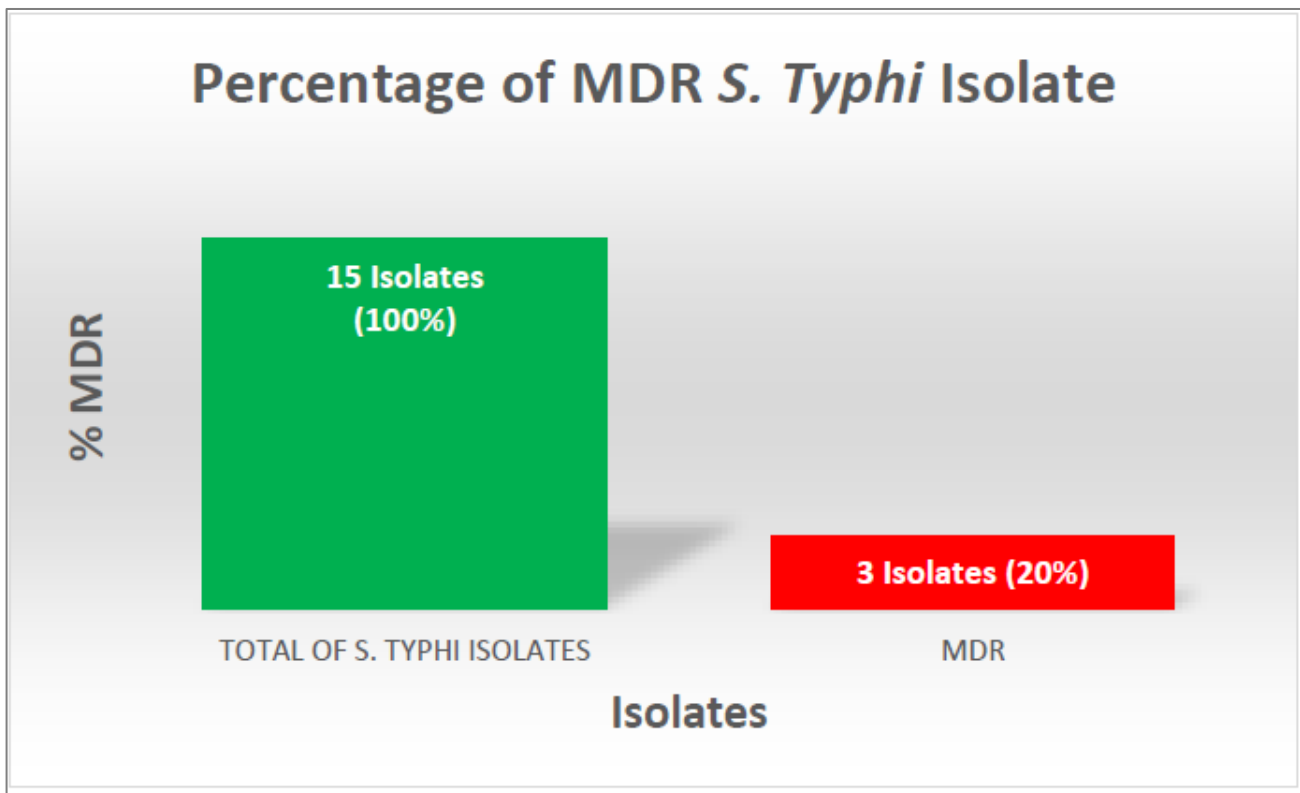


Figure 2: Percentage (%) of MDR Isolates

Methanol was extracted using the methodology described by Willie *et al.* (2021). Each plant sample was weighed out to five (5) grams and added to the extraction thimble of a Soxhlet extractor. To aid in the sample's dissolution, approximately 50 mL of a methanol-dimethyl sulfoxide solvent was added to a round-bottom flask attached to the extractor. The extract obtained from the three reflux cycles was concentrated in a rotary evaporator to a final

volume of 2 mL. The 2 mL extract was then placed into a screw-cap vial labelled appropriately. The 2 millilitre extract was run over a chromatographic column loaded with anhydrous sodium sulfate and well-baked silica gel to produce a pure extract and remove water. The final product was labeled and stored in desiccators at room temperature. The % yield of the extract was computed using a formula described by Tembe Fokunang *et al.* and

Truong et al. (2019, 2021). Percentage yield =  $(Wt \div W0) \times 100$  Where Wt represents the weight of the crude extract obtained, and W0 represented weight of the initial powder.

**Table 1: Bio-screening for Antibacterial Activity against MDR *S. Typhi***

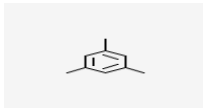
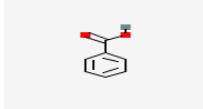
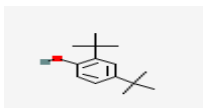
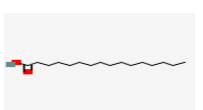
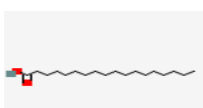
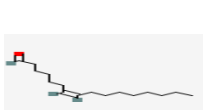
S/N	Plant Extract	Zone of Inhibition (mm)		MIC (mg/mL)	MBC (mg/mL)
		Minimum (50mg of Extract)	Maximum (200mg of Extract)		
1	<i>Vernonia amygdalina</i> (Bitter Leaf)	11	14	50	100
2	<i>Psidium guajava</i> (Guava)	10	13	100	150
3	Concoction ( <i>V. amygdalina</i> + <i>P. guajava</i> )	14	18.5	50	50

**Table 2: Qualitative Phytochemical Analysis Results**

Plant Extract	Alkaloids	Flavonoids	Tannins	Terpenoids	Saponins	Glycosides	Steroids
<i>V. amygdalina</i>	++	++	+++	++	+	++	+
<i>P. guajava</i> (Guava)	+	+++	++	+	++	+	-
CONCOCTION	+	+	+	+	+	+	+

Key: Qualitative analysis: +++ = Strongly present, ++ = moderately present, + = weakly present, - = absent

**Table 3: GC-MS Analysis of (Guava) Extract**

Peak Number	Retention Time (min)	Area %	Identified Compound	Chemical Structure
3	5.387	2.83	Mesitylene	
16	8.219	0.76	Benzoic acid	
27	13.018	0.61	2,4-Di-tert-butylphenol (DTBP)	
38	17.983	9.17	n-Hexadecanoic acid (Palmitic acid)	
46	19.903	9.12	Octadecanoic acid (Stearic acid)	
50	21.104	0.21	cis-11-Hexadecenal	

**Bio-screening of Plant Extracts for Antibacterial Activity**

Mueller-Hinton agar plates were prepared as per the manufacturer’s specifications. Each plant extract was tested for antibacterial efficacy by using the disc diffusion method (Ahman et al., 2022). The test was performed using appropriate control (standard) procedures. In order to do perform the test, the test organism was first activated. This was achieved by sub-culturing in nutrient

broth. This was placed in an incubator at 37°C for 24 hours. A sterile swab was used to spread the 0.1 mL suspension of the activated organism over the surface of Mueller-Hinton agar. Plant extracts were taken at various concentrations and placed on sterile filter paper discs (6 mm in diameter). The plates were incubated at 37°C for 24 hours, and the zone of inhibition of the discs was measured in millimetres. Tests were performed in triplicate, and the mean diameter of the inhibition zones

was recorded. The extracts were prepared serially diluted for the determination of Minimum Inhibitory

Concentration (MIC) values. MIC is the lowest concentration that shows a clear zone of inhibition.

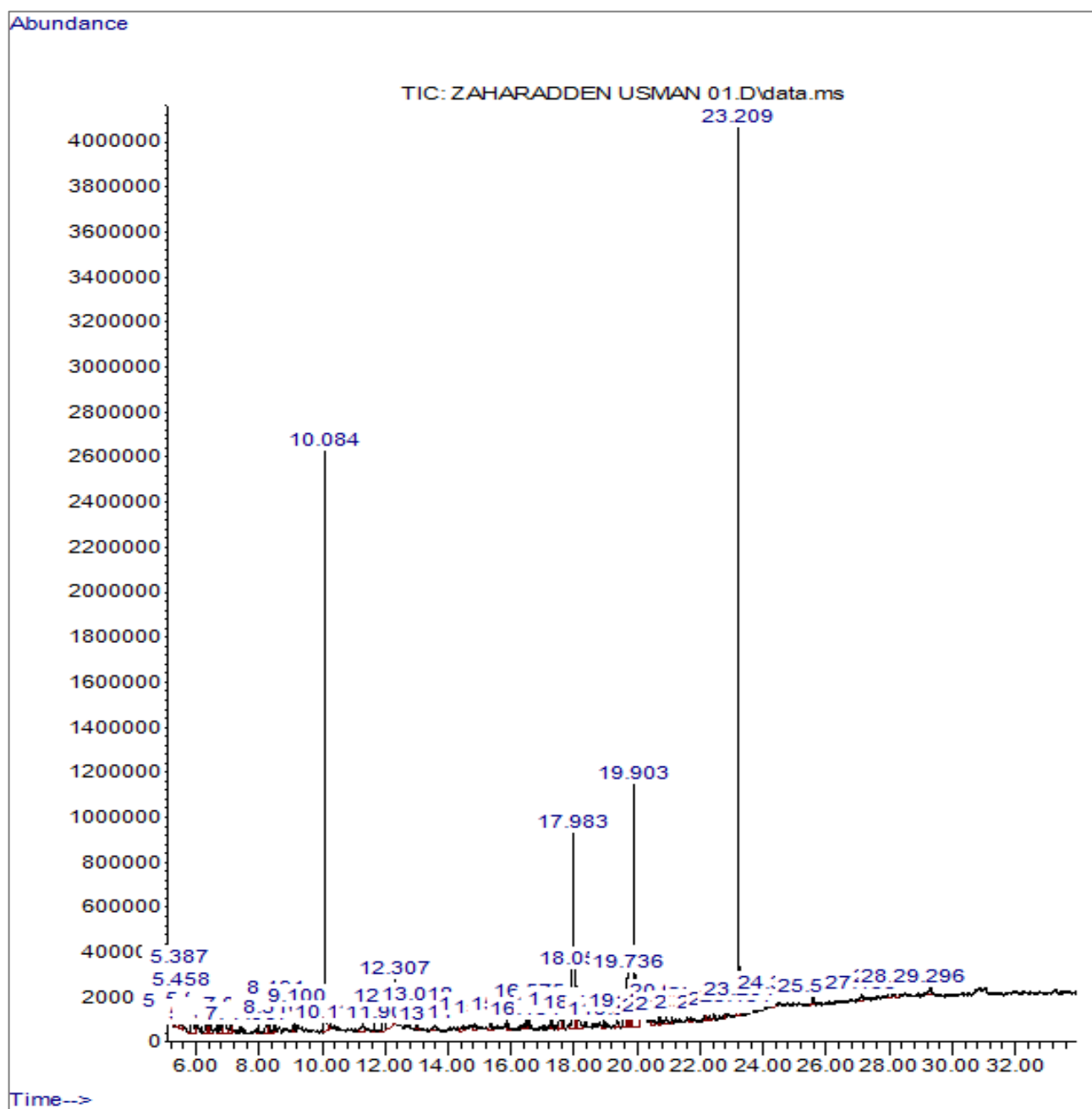


Figure 3 Gas Chromatography–Mass Spectrometry (GC–MS) Total Ion Chromatogram (TIC) of Guava

The Minimum Bactericidal Concentration was determined by subculturing from the samples of those tubes that showed no visible growth in the MIC test on fresh nutrient agar. The plates were incubated again at 37°C for 24 hours, and the lowest concentration that did not show bacterial growth was recorded as the MBC.

#### Qualitative Phytochemical Screening

Phytochemical analysis was the systematic examination and identification of phytochemicals found in plant components, including alkaloids, flavonoids, terpenoids, saponins, tannins, and phenolic compounds. It aided researchers in identifying bioactive compounds, understanding medicinal properties, drug discovery, and

evaluating plant quality in herbal products, supplements, and traditional medicines.

Phytochemical screening was performed on the methanol and aqueous extracts using the following procedures (Dubale *et al.*, 2023). A few drops of diluted sulfuric acid were added to a small amount of each extract. The development of an orange colour indicated the presence of flavonoids. Two drops of Mayer’s reagent were added to a few millilitres of each extract on the side of the test tube. The appearance of a green precipitate confirmed the presence of alkaloids. Two millilitres of each extract were mixed with 2 mL of acetic anhydride and concentrated sulfuric acid. The formation of blue-green rings indicated the presence of terpenoids. 10 mL of distilled water was added to each extract, and the mixture was shaken for 10

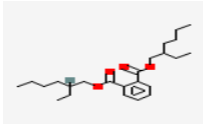
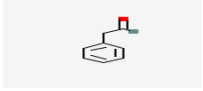

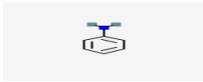
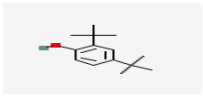
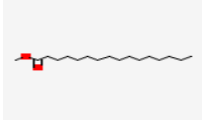

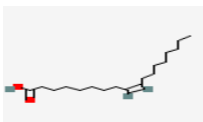
minutes. Form layers stable at around 1 cm in size indicated the presence of saponins. 2 mL of the extract was added to 2 mL of chloroform and 2 mL of acetic anhydride, and a reddish-brown solution formed. A violet-to-blue-green colouration appeared upon the addition of 1 mL of concentrated sulfuric acid and indicated the steroids' presence. Two millilitres (mL) of each extract were mixed with 2 mL of chloroform and 2 mL of acetic anhydride. The formation of a violet to blue-green or reddish-brown ring indicated the presence of glycosides.

#### Quantitative Phytochemical Analysis Using Gas Chromatography-Mass Spectrometry

According to [Chen et al. \(2023\)](#), mass spectrometry (MS) for the identification and quantification of chemical constituents in plant extracts has been a trusted analytical

method for some time. Gas chromatography with a mass spectrophotometric detector attachment, following [Wallie et al., \(2021\)](#) guidelines, where an auto-sampler was used to separate the components of the abstracts as per their volatility. After dilution to about 1 mL, the sample in the split mode with a split ratio of 10: 1 was injected automatically into a GC column. The sample was injected onto a stationary GC column using helium, an inert gas. Keeping the column head pressure at 20 psi yielded a constant flow rate of 1 mL/min. Thermal profile of the column after 1 minute at 55 C for 1 minute; the temperature in the column progressively decreased at a rate of 25 deg C per minute. The temperature then rose to 280°C at 8°C/min, then to 300°C at 25°C/min, and was kept there for 2 minutes. The ion source was heated to 200°C; the contact temperature was 250°C. Full-scan mode at 70 eV yielded mass spectra of the nutrient over m/z 35–550.

**Table 4: GC-MS Analysis of *Vernonia amygdalina* Extract**

Peak Number	Retention Time (min)	Area %	Identified Compound	Chemical Structure
41	23.205	8.58	Bis(2-ethylhexyl) phthalate	
4	6.264	5.40	Benzeneacetaldehyde	
30	18.051	5.21	Dibutyl phthalate	
1	5.212	4.98	Aniline	
14	13.015	2.73	2,4-Di-tert-butylphenol (DTBP)	
27	17.626	2.69	Hexadecanoic acid, methyl ester (Methyl palmitate)	
33	19.692	2.03	9-Octadecenoic acid, (E)- (Elaidic acid)	
34	19.736	1.96	Oleic Acid	

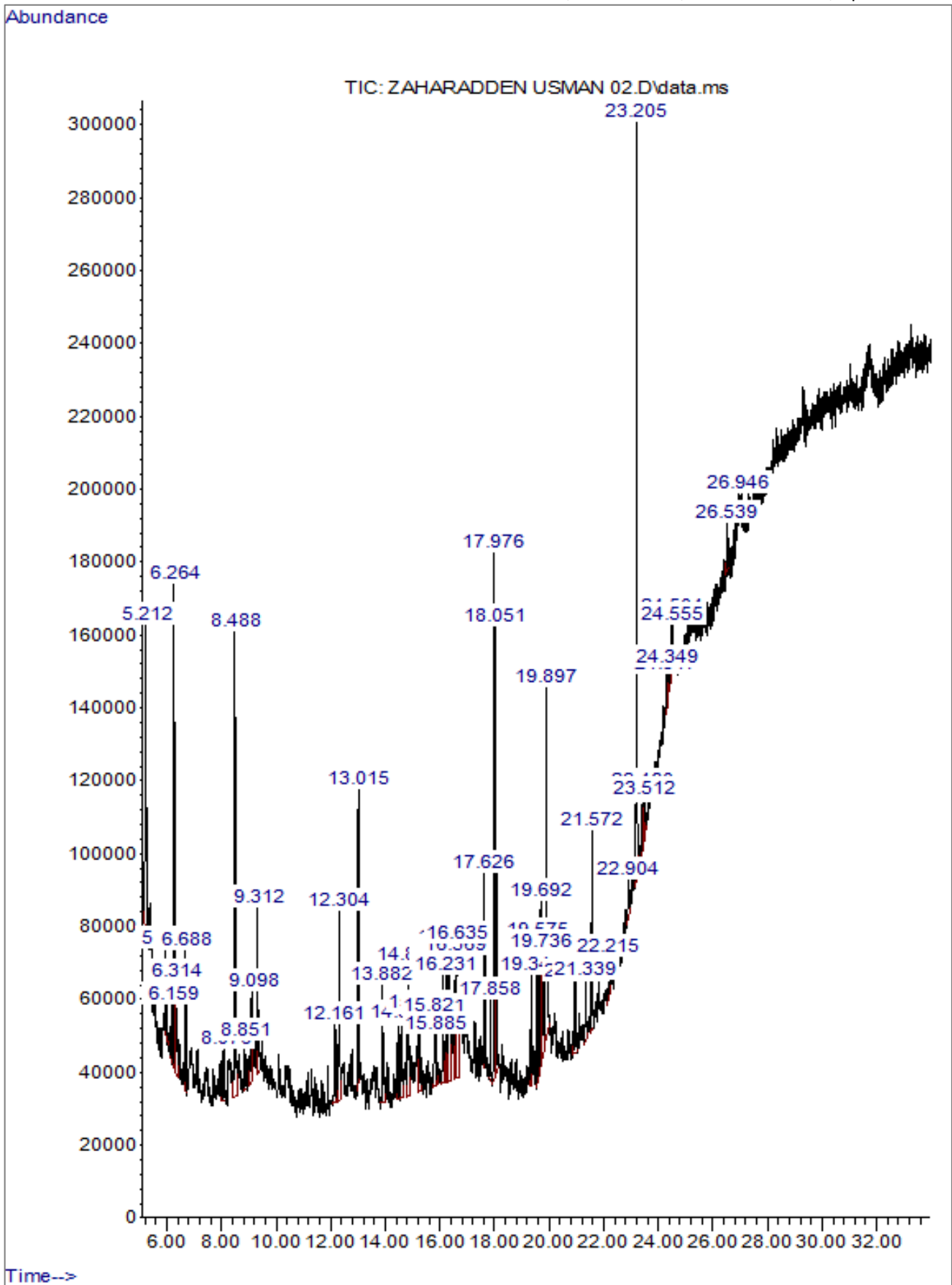
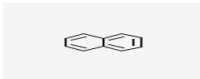
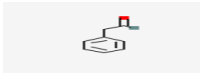

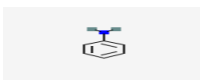

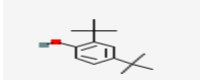

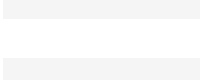


Figure 4 Gas Chromatography–Mass Spectrometry (GC–MS) Total Ion Chromatogram (TIC) of *V. amygdalina*

To identify the phytochemical compounds present in the extract, the retention times of the phytochemicals were compared with those of authentic standards and a mass spectral library from the National Institute of Standards

and Technology (NIST). The retention time of each column component was used to determine the elution order. Elements with lower retention time are eluted before those with higher retention.

**Table 5: GC-MS Analysis of Concoction *V. amygdalina* and *P. guajava***

Peak Number	Retention Time (min)	Area %	Identified Compound	Chemical Structure
9	8.489	9.00	Naphthalene	
5	6.272	6.47	Benzeneacetaldehyde	
36	23.204	8.53	Bis(2-ethylhexyl) phthalate	
1	5.221	5.19	Aniline	
3	5.959	3.68	Limonene	
15	13.016	2.74	2,4-Di-tert-butylphenol (DTBP)	
4	6.171	1.40	Benzyl alcohol	
2	11.897	1.37	Caryophyllene	

#### Fourier Transforms Infrared Spectroscopy (FTIR)

Fourier transform infrared spectroscopy (FTIR) was a successful analytical method for determining and identifying the functional groups present in plant extracts or phytochemicals. The examination of infrared absorption patterns is a non-destructive technique for disclosing the molecular structure of various substances. According to Sosa (2025), oven-dried leaves at 50 °C were ground to a fine powder for FTIR analysis. In a 1:50 ratio, the resultant powder was mixed with potassium bromide to form pellets. A uniform pellet thickness was obtained by applying consistent pressure during preparation. A FTIR spectrophotometer with a resolution of 4 cm<sup>-1</sup> was used to give FTIR spectra in the spectral region of 400–4000 cm<sup>-1</sup>. Each spectrum represented the average of ten scans.

#### Toxicity Studies of the Plant Extract

Healthy, non-pregnant, nulliparous female Wistar rats (120-150 g, 8-12 weeks old) were used in this study. The animals were sourced from the breeding colony of the Faculty of Veterinary Medicine, University of Ibadan, Nigeria, and housed in the animal facility of the Biochemistry Department, Umaru Musa Yar'adua University Katsina (UMYUK). All procedures involving animals were conducted in accordance with the OECD Guideline 425 (Acute Oral Toxicity) and established protocols from previous studies (Dandashire *et al.*, 2019; Sundaram *et al.*, 2021; Ajegi *et al.*, 2023). The rats were acclimatized for seven days under standard laboratory conditions (12 h light/dark cycle, 23–25°C, 40–70% humidity) with free access to a standard rodent diet and water. The toxicity study was performed in two phases: acute (single-dose) and subchronic (28-day repeated-dose).

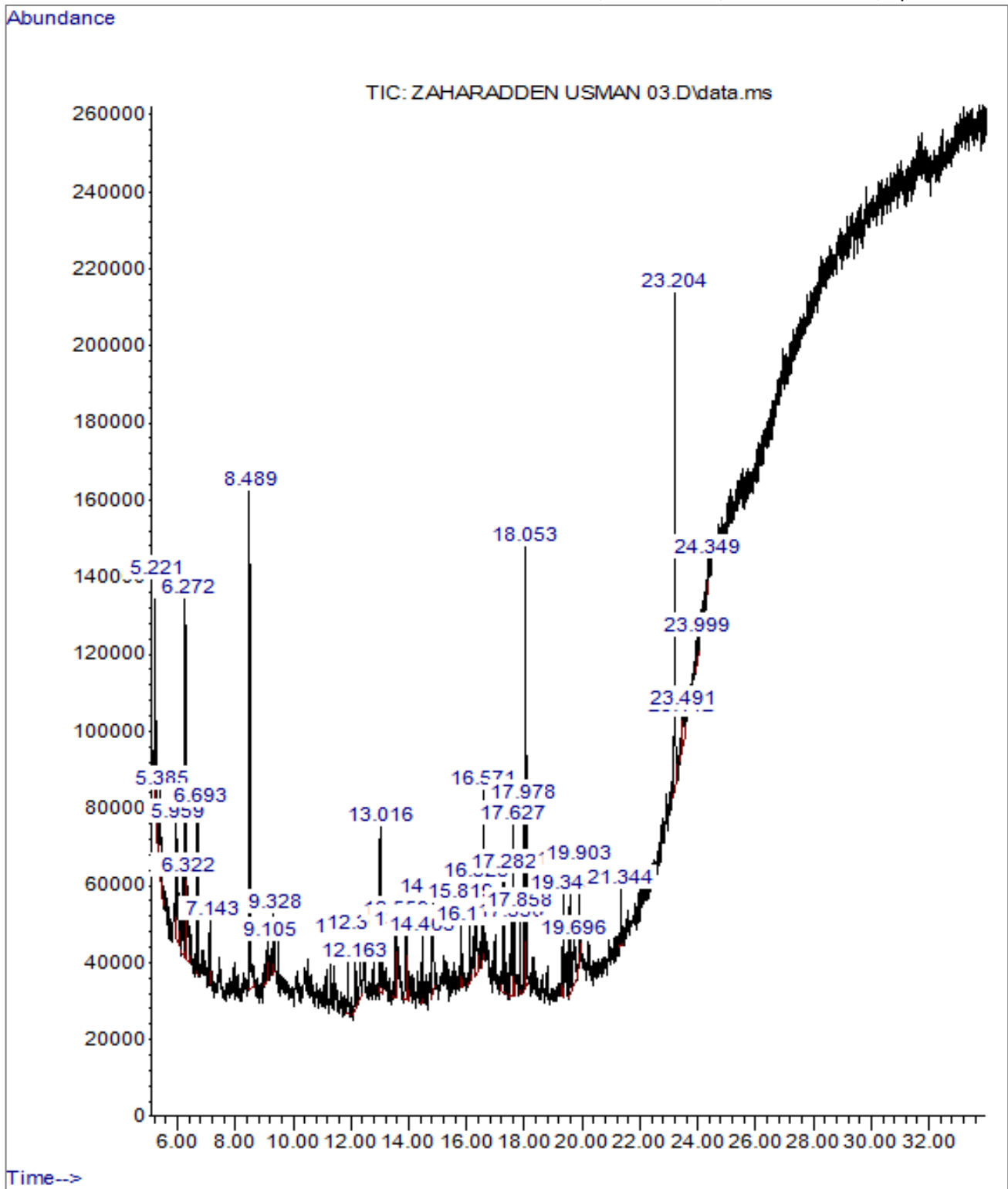


Figure 5 Gas Chromatography–Mass Spectrometry (GC–MS) Total Ion Chromatogram (TIC) of *P. guajava* and *V. amygdalina* Leaf Extract Concoction

**Experimental Animals**

For the study, 36 albino rats weighing 120-150 g and 8-12 weeks old were used, as per Dandashire *et al.* (2019). The normal environmental parameters were maintained in the animal facility during the research, including a 12-hour light/dark cycle, a temperature range of 23°C – 25°C, and humidity between 40 – 70% (or as per the particular species' requirements). The rats were fed a standard rodent diet and had constant access to water for

experimental use. Before the commencement of the trial, there was a seven-day adaptation time.

**Acute Toxicity Studies (initial phase)**

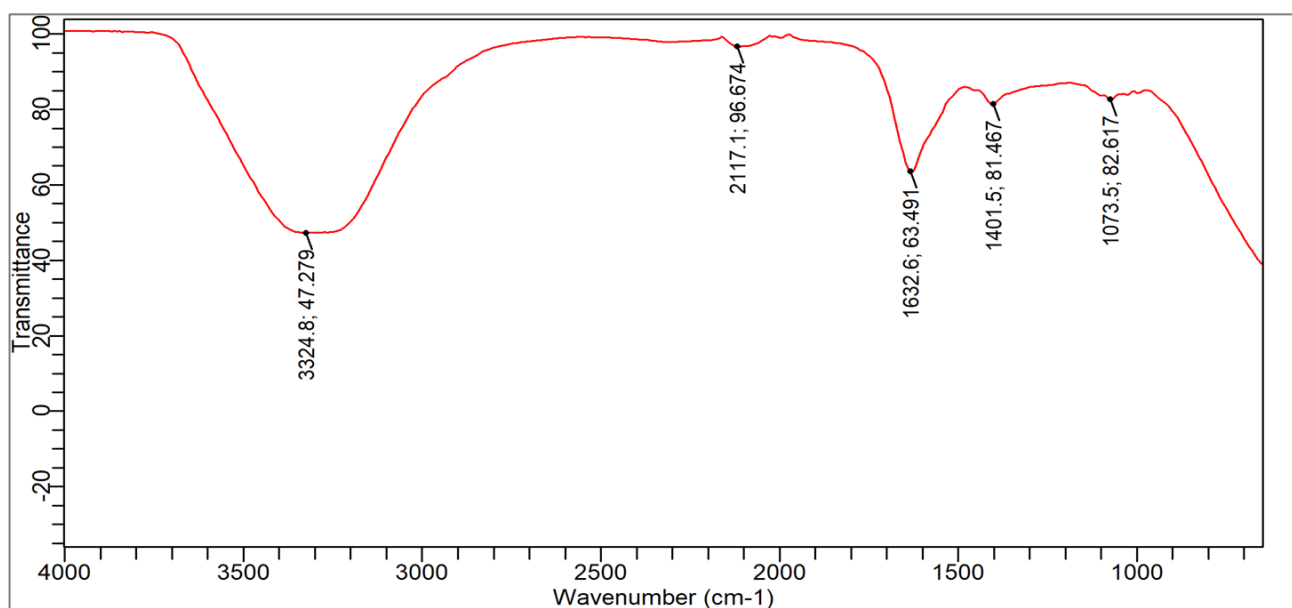
A total of four mice were selected at random. They were assigned to two groups of two mice each. The test group was group A, while the control group was group B. The mice were divided into two groups and kept in separate cages, with a brief overnight fasting period. The plant extract solution was prepared in sterile distilled water at a

specific concentration (mg/kg body weight) and was orally administered once to each mouse in group A. Mice in Group B received normal saline as a negative control. The mice were continuously monitored for a total of 48 hours, first for the first 12 hours and then for signs of toxicity. Monitoring for the manifestation of toxicity was performed as per Sisay et al. (2021). It includes monitoring behavioural disturbances such as alertness,

restlessness, irritability, and fearfulness. Further, in the autonomic response, there are salivation, tears, sweating, piloerection, enuresis, and defecation. Also, in the neurological response, monitor spontaneous activity, reaction time, response to touch, pain sensitivity, seizures, agitated behaviour, and motor activity oscillation. Moreover, monitor for anorexia, morbidity-mortality and other toxicity.

**Table 6: FTIR Spectroscopy Analysis of *Vernonia amygdalina***

Peak Number	Wave number (cm <sup>-1</sup> )	Intensity (%)	Possible Functional Group	Type of Vibration
1	3324.79	47.28	O-H / N-H	Stretching
2	2117.13	96.67	C≡N / C≡C	Stretching
3	1632.57	63.49	C=O (carbonyl) / C=C	Stretching
4	1401.48	81.47	C-H /C-O C-O	Bending
5	1073.47	82.62	(Alcohols/ethers)	Stretching



**Figure 6: Infrared Spectrum of *Vernonia amygdalina***

**Sub-chronic Toxicity Studies (second phase)**

After the first stage, the inquiry entered the second stage. At this point, eight rats were randomly selected and weighed, then divided into four groups of two each. For 28 days, the second, third, and fourth participants received a single oral dose daily of three (3) different concentrations of the extract at mg/kg body weight. The first one (1st), who was controlling, received 2 mL of normal saline daily. Each day, the dosage schedule remained the same; weekly adjustments were made based on changes in the animals’ weights. The rats were provided with sufficient food and water, and they were checked regularly for any abnormal symptoms, diseases, or deaths.

**Assessment of Liver Function Test**

As the final step in the 28-day sub-chronic toxicity study, the animals underwent a night-long fast. After that, euthanasia took place on the 29th day. We used EDTA and lithium heparin vials to quickly draw blood for biochemical investigations. The study included automated assessment of serum protein levels, serum bilirubin, alkaline phosphatase (ALP), aspartate aminotransferase

(AST), and alanine aminotransferase (ALT). The assessment techniques adopted in this study were based on the standards of Dandashire et al. (2019).

**Histopathological Investigations and Microscopic Examinations**

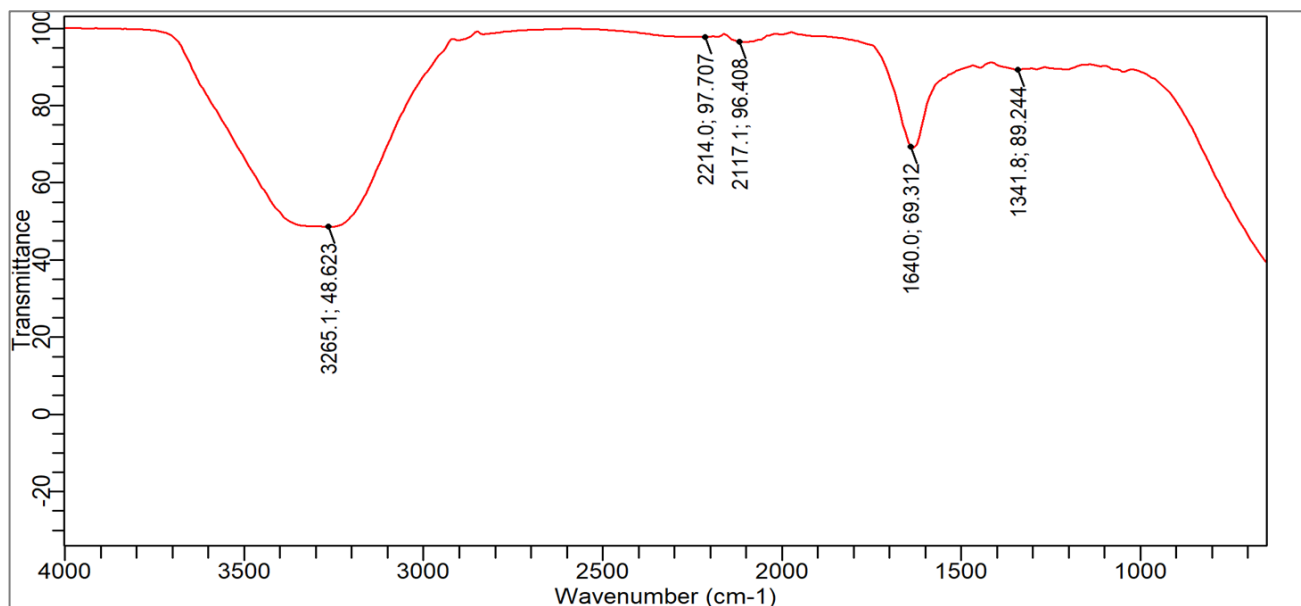
Histopathological analyses were carried out as per the protocols of Dandashire et al. (2019) and Sundaram et al. (2021). Organs such as the kidneys and liver were removed, cut open, and preserved in a solution of 10% formaldehyde. For each tissue, a permanent mount was prepared. The liver and both kidneys of each rat were processed using standard histological methods. Tissues were first dehydrated using different alcohol concentrations (30%, 50%, 70%, and 90%). The tissues were immersed twice in 100% alcohol in order to remove all moisture. Toluene can be used to clean tissues, enhancing the transparency and visibility of inclusions. Following that, the infiltration and embedding processes were accomplished using liquid paraffin and molten paraffin wax, respectively, followed by a Toluene clean, during which the tissues were cleaned to enhance their transparency and the visibility of inclusions. Then, using

L-shaped moulds, infiltration and embedding were carried out with liquid paraffin and molten paraffin wax, respectively. For the preparation of tissue sections, a Rotary Microtome was used, and slides were prepared

using the Hot Plate Method. The tissue sections were stained with eosin and hematoxylin. A microscope with a 40x objective lens was used to view the slides, and photographs were taken.

**Table 7: FTIR Spectroscopy Analysis of *Psidium guajava***

Peak Number	Wavenumber (cm <sup>-1</sup> )	Intensity (%)	Possible Functional Group	Type of Vibration
1	3265.15	48.62	O-H / N-H	Stretching
2	2214.04	97.71	C≡N / C≡C	Stretching
3	2117.13	96.41	C≡C / N=C=O	Stretching
4	1640.03	69.31	C=O(carbonyl)/C=C	Stretching
5	1341.84	89.24	C-H / C-O	Bending



**Figure 7: Infrared Spectrum of *Psidium guajava***

**Bioinformatic Analysis of the Plant Extract**

Using the internet resource DAVID (<https://david.ncicrf.gov/>), the possible biological pathways and processes connected to the bioactive compound's anti-*S. Typhi* activities were examined in accordance with the protocol described Han *et al.* (2024). Gene ontology (GO) and Kyoto Encyclopedia of Genes and Genomes (KEGG) pathway enrichment analysis were performed on common targets. Genes were categorized by gene ontology annotation into three groups: cellular component (CC), molecular function (MF), and biological process (BP). KEGG analysis aided the comprehension of gene regulation networks (Xu *et al.*, 2024). Using the logarithm of p-values helped with the categorization and visualization of KEGG pathways and GO keywords (Zhang *et al.*, 2020)

**Molecular Docking**

Assessing the binding affinities of active substances and targets. Core targets and important bioactive chemicals were selected using molecular docking methods described by Agu *et al.* (2023). The PDB database (<https://www.rcsb.org/>) was the initial source of the target proteins' structure files. Following the removal of organic molecules and solvents with PyMOL software, the protein structure files were converted to pdbqt format

using the Auto-Dock 4.2 program package (<http://autodock.scripps.edu/>), which included the inclusion of hydrogen and charge computation. Using the Open Babel program, the 3D structure files of bioactive substances were retrieved and transformed to the pdbqt format. The Auto-Dock Vina software was used to perform the docking, and grid box data from the Getbox plugin in PyMOL were used. The binding conformations with the lowest binding energy were chosen and compared.

**RESULTS**

**Antibiotic Susceptibility Profile of *S. Typhi* Isolates to Screen MDR Strains**

Fifteen (15) clinical isolates of *Salmonella enterica serovar Typhi* were tested against three first-line antibiotics from different classes. This antibiotic susceptibility profile indicates a considerable degree of resistance among the *S. Typhi* isolates, with almost half (46.7%) exhibiting resistance to ciprofloxacin, whereas a lower proportion were resistant to ceftriaxone (20%) and azithromycin (13.3%), as shown in Figure 1, resulting in three isolates (20% of the specimens) being designated as multi-drug resistant (Figure 2).

Table 8: FTIR Spectroscopy Analysis of *P. guajava* + *V. amygdalina*

Peak Number	Wavenumber (cm <sup>-1</sup> )	Intensity (%)	Possible Group	Functional	Type of Vibration
1	3324.79	59.23	O-H / N-H		Stretching
2	2117.13	97.30	C≡N / C≡C		Stretching
3	1632.57	70.83	C=O (carbonyl) / C=C		Stretching
4	1401.48	87.38	C-H / C-O		Bending
5	1237.48	89.53	C-O / C-N		Stretching
6	1073.47	86.64	C-O (alcohols)		Stretching

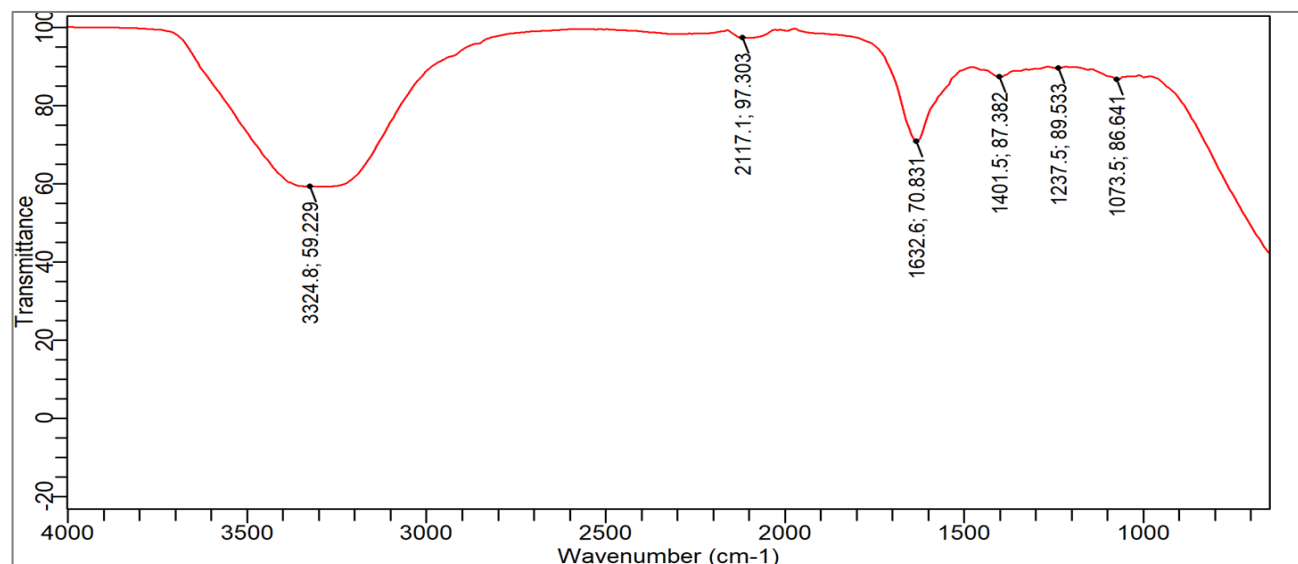
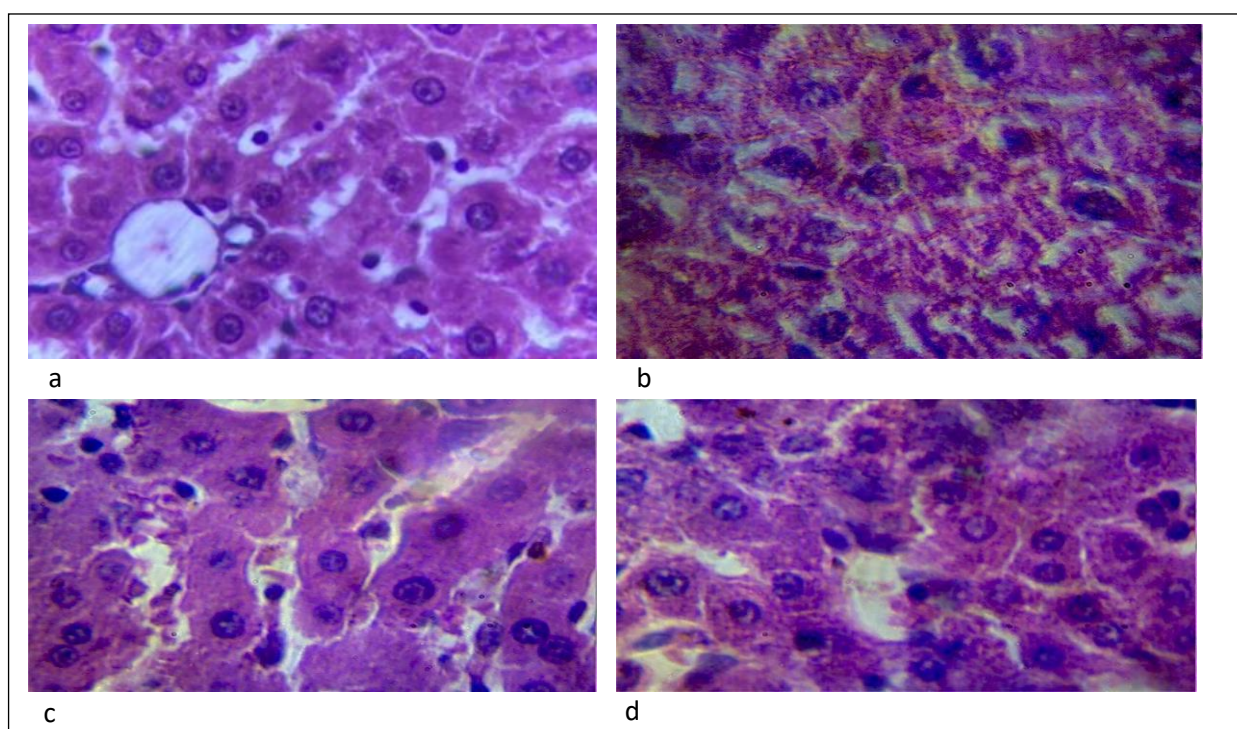

 Figure 8: Infrared Spectrum of concoction (*P. guajava* and *V. amygdalina*)

Table 9: Correlation of FTIR Spectroscopy Results

Functional Group & Vibration	<i>V. amygdalina</i>	<i>P. guajava</i>	Concoction	Correlation & Interpretation (Enders <i>et al.</i> , 2021)
O-H / N-H Stretching ~3325 cm <sup>-1</sup>	Strong (47.28%)	Strong (48.62%)	Strongest (59.23%)	The Concoction shows an <b>enhanced signal</b> , indicating a higher concentration or diversity of phenolic compounds (e.g., tannins, flavonoids), suggesting a synergistic blend.
C≡N / C≡C Stretching ~2117 cm <sup>-1</sup>	Very Strong (96.67%)	Very Strong (96.41%)	Very Strong (97.30%)	A <b>highly consistent</b> dominant peak across all three, indicating nitriles or alkynes are a core, shared component of the antimicrobial phytochemical profile.
C=O / C=C Stretching ~1632-1640 cm <sup>-1</sup>	Strong (63.49%)	Strong (69.31%)	Strong (70.83%)	<b>Consistently present</b> in all samples, confirming abundant carbonyls (in acids, ketones) and alkenes, fundamental to flavonoids and terpenoids.
C-H Bending / C-O ~1341-1401 cm <sup>-1</sup>	Strong (81.47%)	Strong (89.24%)	Strong (87.38%)	A <b>prominent and shared</b> feature, confirming the complex organic nature and presence of alkanes and alcohols in all extracts.
C-O / C-N Stretching ~1237 cm <sup>-1</sup>	Not Reported	Not Reported	Strong (89.53%)	A <b>distinct, new peak unique to the Concoction</b> . This

**Table 10: Acute Toxicity Evaluation of *V. amygdalina* and *P. guajava* Extracts in Wistar Albino Rats**

Group	Treatment	Dose (mg/kg)	No. of Rats	Mortality	Observations
A1	<i>V. amygdalina</i>	250	3	0	Normal
A2	<i>V. amygdalina</i>	500	3	0	Mild sedation
A3	<i>V. amygdalina</i>	1000	3	0	Reduced activity
B1	<i>P. guajava</i>	250	3	0	Normal
B2	<i>P. guajava</i>	500	3	0	Normal
B3	<i>P. guajava</i>	1000	3	0	Slight lethargy
C1	Concoction	250	3	0	Normal
C2	Concoction	500	3	0	Mild sedation
C3	Concoction	1000	3	0	Decreased activity
Cn1	Control	2ml	3	0	Normal
Cn2	Control	2ml	3	0	Normal
Cn3	Control	2ml	3	0	Normal



**Figure 9: Representative photomicrographs of Kidney sections from Wistar rats treated with (a) Normal saline (as a positive control), (b) 250 mg/kg of *Vernonia amygdalida*, (c) 500 mg/kg of *Vernonia amygdalida* and (d) 1000 mg/kg of *Vernonia amygdalida***

#### Bio-screening for Antibacterial Activity against MDR *S. Typhi*

The antibacterial screening (Table 1) showed that a mixture of *Vernonia amygdalina* and *Psidium guajava* was the most potent, exhibiting a synergistic effect with the greatest inhibition zone and the lowest required bactericidal dose, followed by *Vernonia amygdalina* and *Psidium guajava*.

#### Qualitative Phytochemical Analysis of the Plants Extract

The qualitative phytochemical screening (Table 2) revealed distinct and complementary profiles for the plants, *V. amygdalina* and *P. guajava*. *V. amygdalina* exhibited the strongest tannin content (+++), along with moderate levels of alkaloids, flavonoids, terpenoids, and glycosides, and a weak presence of saponins and steroids.

In contrast, *P. guajava* is characterized by a very strong (+++) flavonoid content. It also contained moderate tannins and saponins, but was notably devoid of steroids. The concoction (mixture of *V. amygdalina* and *P. guajava*) presented a unique, balanced profile. It contained a weak to moderate (+) presence of all phytochemical classes tested, including steroids.

#### GC-MS Analysis of *Psidium guajava* Extract

The GC-MS analysis of Guava (Table 3 and Figure 3) revealed a complex chemical profile, with Bis(2-ethylhexyl) phthalate (23.23%) as the dominant compound, followed by a significant presence of fatty acids including an unidentified peak at 14.06%, Palmitic acid (9.17%), and Stearic acid (9.12%), alongside minor constituents such as Mesitylene and 2,4-Di-tert-butylphenol, indicating a lipid-based sample potentially contaminated with a synthetic plasticizer.

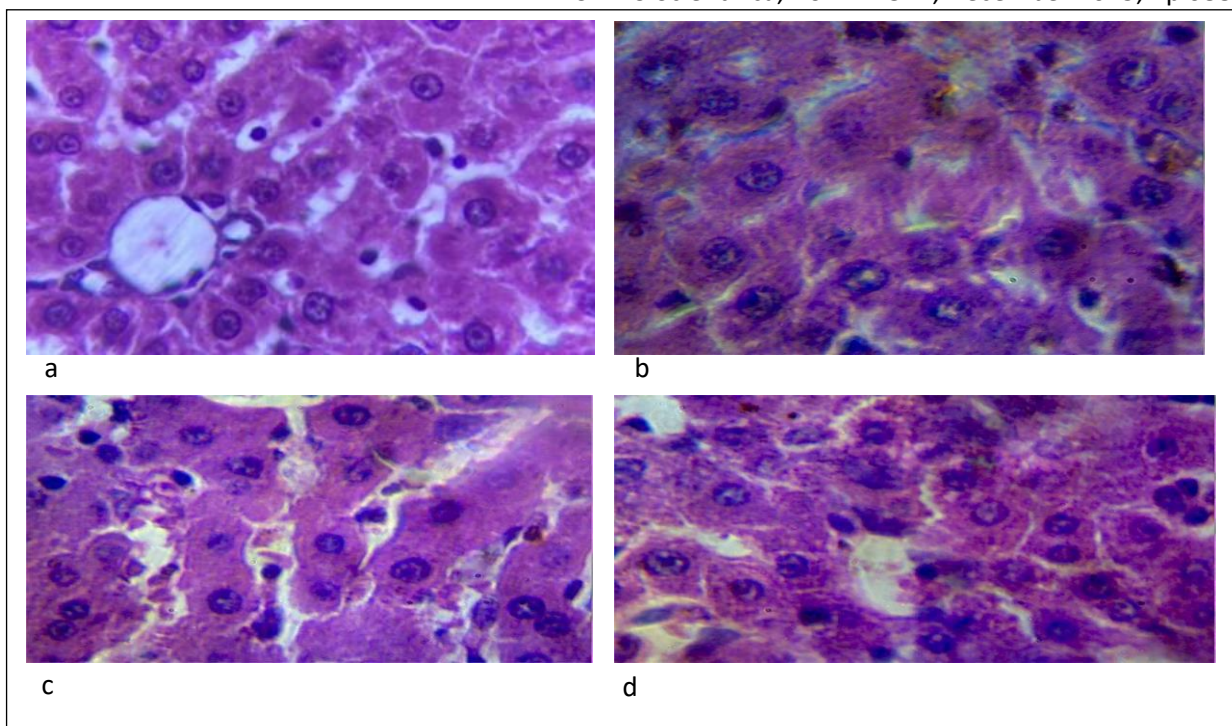


Figure 10: Representative photomicrographs of Kidney sections from Wistar rats treated with (a) Normal saline (as a positive control), (b) 250 mg/kg of *Psidium guajava*, (c) 500 mg/kg of *Psidium guajava* and (d) 1000 mg/kg of *Psidium guajava*

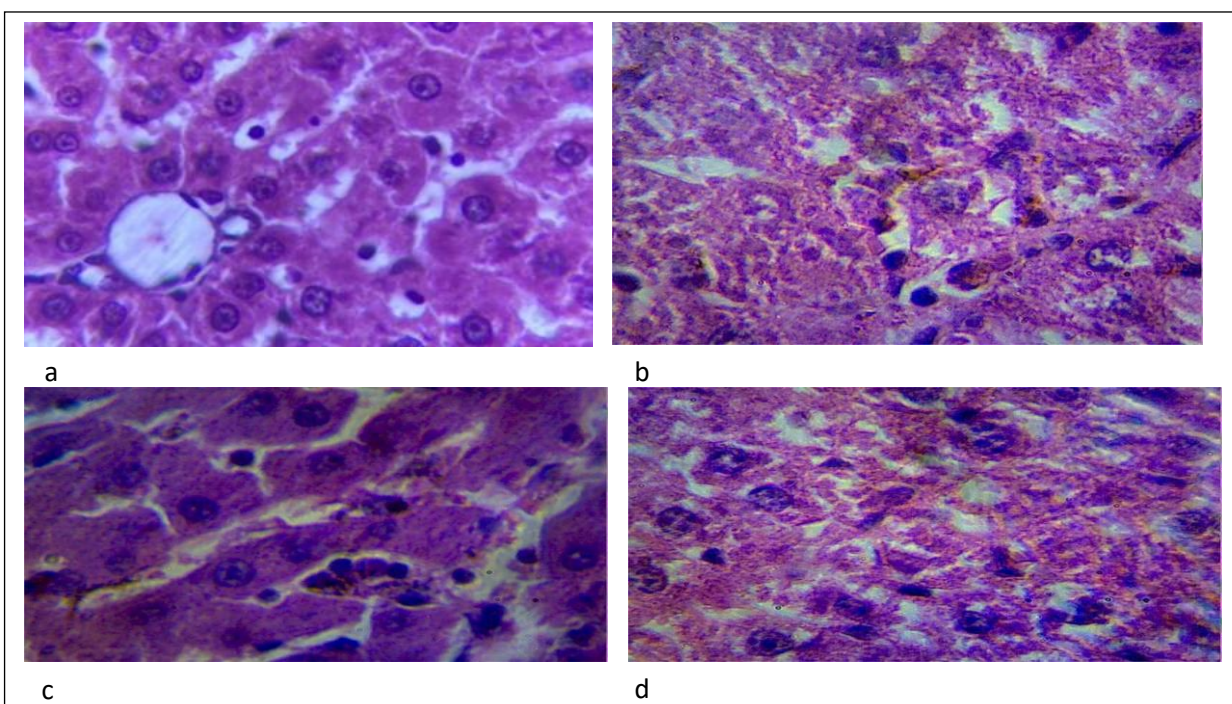


Figure 11: Representative photomicrographs of Kidney sections from Wistar rats treated with (a) Normal saline (as a positive control), (b) 250 mg/kg of Concoction (*P. guajava* and *V. amygdalina*), (c) 500 mg/kg of Concoction (*P. guajava* and *V. amygdalina*) and (d) 1000 mg/kg of Concoction (*P. guajava* and *V. amygdalina*)

#### GC-MS Analysis of *Vernonia amygdalina* Extract

The GC-MS analysis of the *Vernonia amygdalina* extract (Table 4 and Figure 4) showed that the major compound at 8.58 % was Bis(2-ethylhexyl) phthalate. This profile contains large quantities of fatty acid and their derivatives (C<sub>16</sub>H<sub>32</sub>O<sub>2</sub>), n-Hexadecanoic acid (Palmitic acid, 5.96%), Octadecanoic acid (Stearic acid, 4.98%), Esters (2.69%), etc. Interestingly, in addition to that, we also detected

several phthalates (dibutyl and dimethyl phthalate), along with hydrocarbons (Naphthalene, 5.81%) and aldehydes (Benzeneacetaldehyde, 5.40%). The chemical diversity is complemented by the presence of Aniline (4.98%) and the antioxidant 2,4-Di-tert-butylphenol (2.73%). The writing suggests the extract contains natural bioactive lipids. It also indicates possible environmental contamination from plasticizers and industrial chemicals.

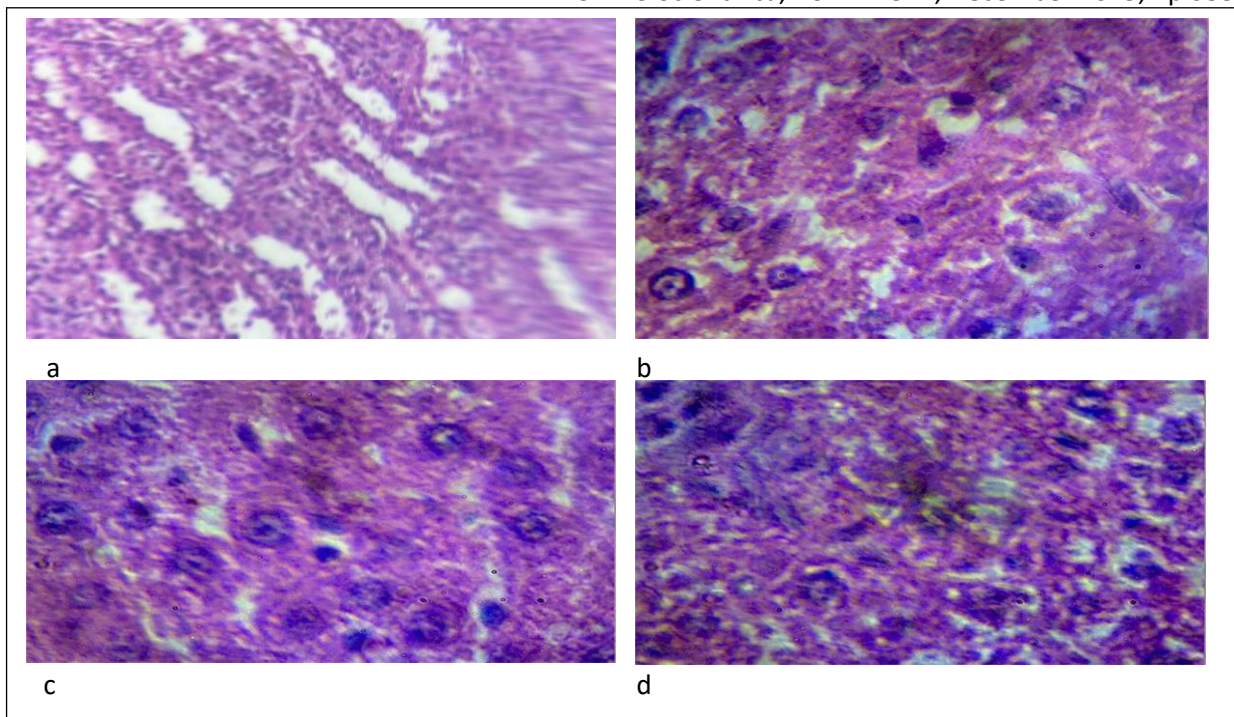


Figure 12: Representative photomicrographs of liver sections from Wistar rats treated with (a) Normal saline (as a positive control), (b) 250 mg/kg of *Vernonia amygdalida*, (c) 500 mg/kg of *Vernonia amygdalida* and (d) 1000 mg/kg of *Vernonia amygdalida*

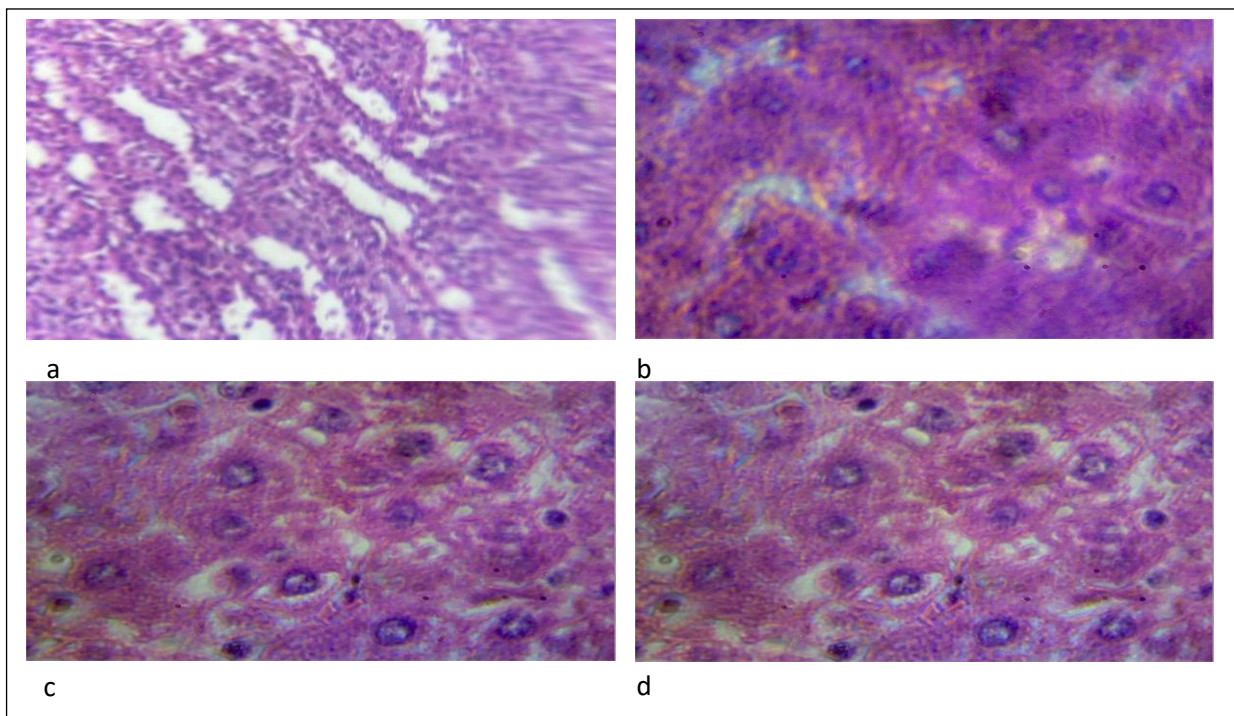
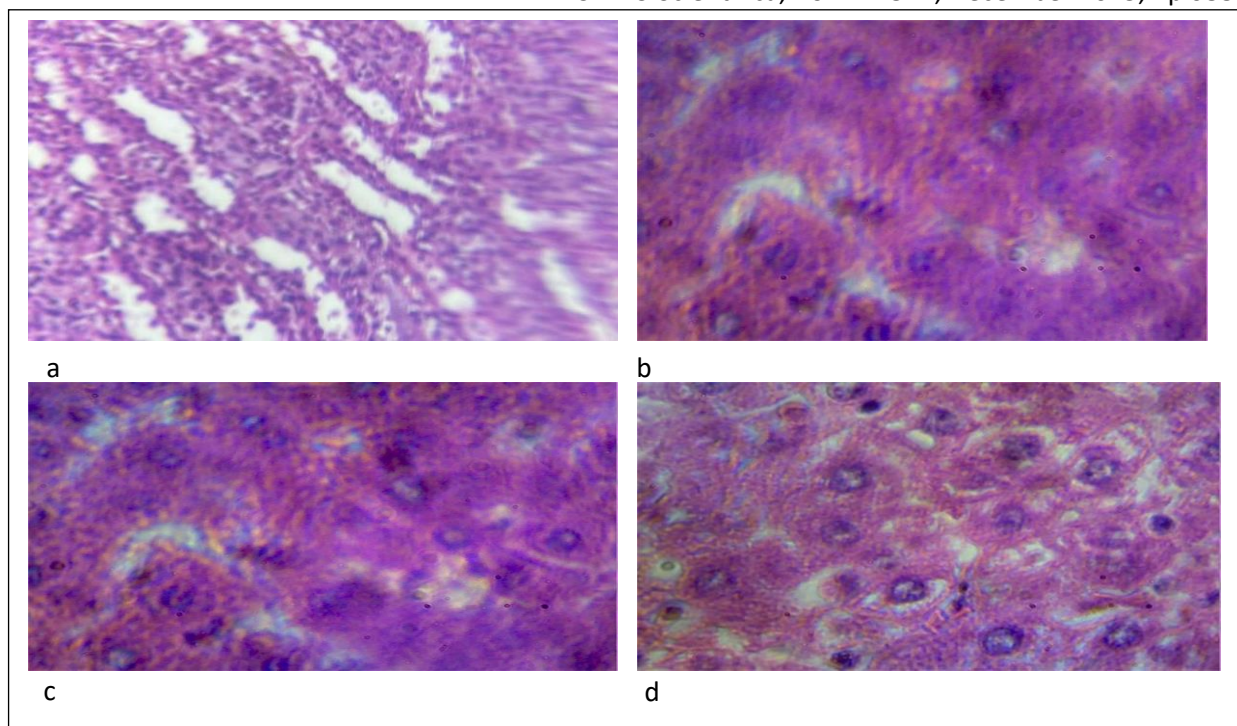


Figure 13: Representative photomicrographs of liver sections from Wistar rats treated with (a) Normal saline (as a positive control), (b) 250 mg/kg of *Psidium guajava*, (c) 500 mg/kg of *Psidium guajava* and (d) 1000 mg/kg of *Psidium guajava*

**GC-MS Analysis of Concoction *V. amygdalina* and *P. guajava***

The *Vernonia amygdalina* and *Psidium guajava* mix (Table 5 and Figure 5) analyzed by GC-MS contains mainly aromatic hydrocarbons and plasticizers. Naphthalene with 9.00% concentration was found in the highest amount, followed by Bis(2-ethylhexyl) phthalate (8.53%)

and Dibutyl phthalate (7.53%). Benzeneacetaldehyde and Aniline were found in high amounts in the chemical constituents. Both these compounds are man-made substances. Other than these, there were also several plant-derived materials found in the chemical makeup of *Phyllanthus amarus*. As this composition contains bioactive plant metabolites, it also shows significant contamination from industrial chemicals and plasticizers.



**Figure 14:** Representative photomicrographs of liver sections from Wistar rats treated with (a) Normal saline (as a positive control), (b) 250 mg/kg of Concoction (*P. guajava* and *V. amygdalina*), (c) 500 mg/kg of Concoction (*P. guajava* and *V. amygdalina*) and (d) 1000 mg/kg of Concoction (*P. guajava* and *V. amygdalina*)

#### FTIR Spectroscopy Analysis of *Vernonia amygdalina*

The FTIR spectroscopic analysis of *Vernonia amygdalina* (Table 6 and Figure 6) detected key functional groups, showing a broad O-H or N-H stretch at  $3324\text{ cm}^{-1}$ , a distinct  $\text{C}\equiv\text{N}$  or  $\text{C}\equiv\text{C}$  stretch at  $2117\text{ cm}^{-1}$ , an intense carbonyl (C=O) or alkene (C=C) stretch at  $1632\text{ cm}^{-1}$ , a prominent C-H bending or C-O vibration at  $1401\text{ cm}^{-1}$ , and a strong C-O stretch characteristic of alcohols or ethers at  $1073\text{ cm}^{-1}$ , together indicating the presence of compounds such as phenols, alcohols, nitriles, alkenes, and carbonyls.

#### FTIR Spectroscopy Analysis of *Psidium guajava*

The FTIR spectroscopic profile of *Psidium guajava* (Table 7 and Figure 7) shows an intricate phytochemical signature, marked by intense, distinct peaks for nitrile ( $\text{C}\equiv\text{N}$ ) or alkyne ( $\text{C}\equiv\text{C}$ ) groups and a pronounced carbonyl (C=O) or alkene (C=C) stretch, accompanied by a broad O-H band suggesting phenols or alcohols and noticeable C-H bending vibrations, together confirming the presence of principal antimicrobial constituents like flavonoids, tannins, and terpenoids, which align with its documented antibacterial activity.

#### FTIR Spectroscopy Analysis of Concoction *P. guajava* + *V. amygdalina*

The FTIR analysis of the Concoction (Table 8 and Figure 8) shows a rich and intricate phytochemical profile, characterized by a broad O-H/N-H stretching vibration suggesting phenolic compounds and alcohols, a very intense and sharp nitrile or alkyne ( $\text{C}\equiv\text{N}/\text{C}\equiv\text{C}$ ) peak, a prominent carbonyl or alkene (C=O/C=C) stretch typical of flavonoids and terpenoids, along with pronounced C-H

bending and distinct C-O stretching vibrations of alcohols, ethers, and possibly carboxylic acids, collectively illustrating the synergistic blend of functional groups from the constituent plants that underlie its enhanced antibacterial activity.

#### Correlation of FTIR Spectroscopy Results

FTIR analysis, as displayed in Table 9, shows that the Concoction is not merely a simple mixture but a synergistic blend, marked by a markedly increased level of phenolic compounds (O-H/N-H) and the appearance of a distinctive, intense peak (C-O/C-N), suggesting the formation of new chemical entities that likely underlie its superior bioactivity relative to the individual extracts of *V. amygdalina* and *P. guajava*.

#### Acute Toxicity Evaluation of *V. amygdalina* and *P. guajava* Extracts in Wistar Albino Rats

The acute toxicity assessment (Table 10) demonstrated a favorable safety profile for both *V. amygdalina* and *P. guajava* extracts and their mixture, as no mortality was observed in any Wistar albino rats across all tested dose levels up to 1000 mg/kg, with only mild and transient behavioral changes such as sedation, reduced activity, and slight lethargy noted at the higher doses, while all control groups remained normal.

#### Toxicity Effect of *Vernonia amygdalina*, *Psidium guajava* and their Concoction in Liver/Kidney

According to the histopathological analysis (Figure 9, 10, 11, 12, 13 and 14), the extracts of *Vernonia amygdalina*, *Psidium guajava*, and their mixture displayed a dose-related toxicity pattern in the liver and kidneys of Wistar rats,

where all treatments showed no severe toxicity at the lowest dose (250 mg/kg). *P. guajava* exhibited the safest profile, showing no adverse effects at 250 mg/kg and only slight alterations at higher doses, while *V. amygdalina* and

the mixture at the top dose (1000 mg/kg) produced moderate yet non-necrotic and non-fibrotic pathological changes, including Kupffer cell activation and mild interstitial nephritis (Table 11).

**Table 11: Toxicity Effect of *Vernonia amygdalina*, *Psidium guajava* and their Concoction (*Vernonia amygdalina*+ *Psidium guajava*) in Liver and Kidney**

Group	Treatment	Dose (mg/kg)	Liver Findings	Kidney Findings	Toxicity Grade
Control (Cn1–Cn3)	Normal saline	2 mL	Normal architecture: No necrosis or inflammation or fatty changes	Normal glomeruli and tubules: No degeneration or inflammation	None
<i>V. amygdalina</i> (A1)	<i>Vernonia amygdalina</i> (Bitter Leaf)	250	Mild sinusoidal dilation: No significant hepatocyte damage	Intact renal corpuscles: No tubular necrosis	Mild
<i>V. amygdalina</i> (A2)	<i>Vernonia amygdalina</i>	500	Focal inflammatory infiltrates: Minimal lymphocyte aggregation	Slight tubular congestion: No glomerular damage	Mild
<i>V. amygdalina</i> (A3)	<i>Vernonia amygdalina</i>	1000	Moderate Kupffer cell activation: No necrosis or fibrosis	Mild interstitial oedema: No significant pathology	Moderate
<i>guajava</i> (B1)	<i>Psidium guajava</i> (Guava)	250	Normal hepatocytes: No pathological changes	Normal renal cortex: No abnormalities	None
<i>guajava</i> (B2)	<i>Psidium guajava</i>	500	Slight vacuolation: No necrosis or inflammation	Minimal tubular dilation: No degeneration	Mild
<i>guajava</i> (B3)	<i>Psidium guajava</i>	1000	Mild centrilobular congestion: No hepatocyte necrosis	Focal tubular casts: No glomerular injury	Mild
Concoction (C1)	<i>V. amygdalina</i> + <i>P. guajava</i>	250	Normal structure: No adverse effects	No lobular histopathological lesions	None
Concoction (C2)	<i>V. amygdalina</i> + <i>P. guajava</i>	500	Mild portal triad inflammation: No fibrosis	Slight tubular congestion: No necrosis	Mild
Concoction (C3)	<i>V. amygdalina</i> + <i>P. guajava</i>	1000	Focal hepatocyte ballooning: No necrosis	Mild interstitial nephritis: No severe damage	Moderate

**Weight Changes of the Albino Rat (Before vs. After 28 days)**

Throughout the 28-day sub-acute toxicity study (Table 12), all treatment groups exhibited slight and non-severe weight changes, with the control group showing a slight average increase of 0.8% while groups administered *V. amygdalina*, *P. guajava*, and their concoction demonstrated mild, dose-dependent weight reductions ranging from 0.7% to 2.9%, which correlated with

transient behavioral observations of reduced activity and sedation but no signs of severe systemic toxicity.

**Biochemical Parameters of the Albino Rats**

Based on the thorough toxicological assessment (Table 13), the study reveals a specific organ-specific safety profile for each treatment at the high dose of 1000 mg/kg: *Vernonia amygdalina* caused mild, dose-related hepatotoxicity and slight renal strain reflected by raised liver enzymes (ALT, AST) and creatinine; the Concoction

showed a comparable but slightly intensified pattern of liver and kidney stress, potentially due to phytochemical interactions; in sharp contrast, *Psidium guajava* exhibited the safest profile with minimal biochemical alterations,

indicating a hepatoprotective effect, and importantly, all treatments showed no adverse effects on hematological parameters, confirming the absence of bone-marrow toxicity or anemia.

**Table 12: Weight Changes the Albino Rat (Before vs. After 28 days)**

Group	Treatment	Dose (mg/kg)	Initial Weight (g)	Final Weight	Weight Change (%)	Observations
Cn1–Cn3 Control	(normal saline)	2 mL	130 ± 5	131 ± 4	+0.8%	No adverse effects
A1	<i>V. amygdalina</i>	250	130 ± 5	128 ± 4	-1.5%	Normal behavior
A2	<i>V. amygdalina</i>	500	135 ± 6	132 ± 5	-2.2%	Mild sedation
A3	<i>V. amygdalina</i>	1000	140 ± 7	136 ± 6	-2.9%	Reduced activity
B1	<i>P. guajava</i>	250	125 ± 4	124 ± 3	-0.8%	Normal behavior
B2	<i>P. guajava</i>	500	128 ± 5	127 ± 4	-0.8%	Normal behavior
B3	<i>P. guajava</i>	1000	132 ± 6	130 ± 5	-1.5%	Slight lethargy
C1	Concoction	250	138 ± 5	137 ± 4	-0.7%	Normal behavior
C2	Concoction	500	142 ± 6	139 ± 5	-2.1%	Mild sedation
C3	Concoction	1000	145 ± 7	141 ± 6	-2.8%	Decreased activity

**Table 13: Biochemical Parameters of the Albino Rat Used**

Parameter	Control (Saline)	Normal Range (Adults)	<i>V. amygdalina</i> (1000 mg/kg)	<i>P. guajava</i> (1000 mg/kg)	Concoction (1000 mg/kg)	Interpretation
ALT (U/L)	35 ± 2	7–56	42 ± 3	38 ± 2	45 ± 4	Mild hepatotoxicity at high doses.
AST (U/L)	40 ± 3	8–48	55 ± 5	48 ± 4	60 ± 6	Elevated AST suggests minor liver stress
ALP (U/L)	120 ± 10	44–147	150 ± 12	130 ± 8	160 ± 15	Biliary function mildly affected.
Total Bilirubin (mg/dL)	0.5 ± 0.1	0.3 – 1.2	0.8 ± 0.2	0.6 ± 0.1	0.9 ± 0.3	No clinical jaundice observed.
Creatinine (mg/dL)	0.6 ± 0.1	0.7 – 1.3	0.9 ± 0.2	0.7 ± 0.1	1.0 ± 0.3	Slight kidney strain at 1000 mg/kg.
Urea (mg/dL)	25 ± 3	7 – 20	35 ± 4	28 ± 2	38 ± 5	Minimal nephrotoxicity.

**Haematological Parameters of the Albino Rat Used**

The biochemical analysis at the high dose of 1000 mg/kg demonstrated that *Vernonia amygdalina* and the Concoction caused mild, reversible hepatotoxicity, shown by elevated ALT, AST, and ALP levels, along with minor renal stress as shown by increased creatinine and urea, whereas *Psidium guajava* exhibited a significantly safer profile with only minimal alterations; nevertheless, all treatments did not produce adverse effects on hematological parameters,

underscoring the lack of bone-marrow toxicity, anemia, or clotting disruption (Table 14).

**Molecular Docking Results of *S. typhi***

Based on the molecular docking results (Table 15 and Figure 15 - 16), the phytochemicals showed variable binding affinities to *S. Typhi* target proteins, with Oleic acid displaying the most potent inhibition of DNA Gyrase (-6.4 kcal/mol) and

Methyl-di-*t*-butylhydroxyhydrocinnamate exhibiting the highest binding affinity toward the sipD protein (-6.6 kcal/mol), indicating their potential as effective anti-typhoidal agents.

**Table 14: Hematological Parameters of the Albino Rat Used (Hematological analysis revealed no clinically adverse effects on blood components)**

Parameter	Control (Saline)	Normal Level (In Adult)	<i>V. amygdalina</i> (1000 mg/kg)	<i>P. guajava</i> (1000 mg/kg)	Concoction (1000 mg/kg)	Interpretation
<b>WBC</b> ( $\times 10^3/\mu\text{L}$ )	6.5 $\pm$ 0.5	4-11	7.0 $\pm$ 0.6	6.8 $\pm$ 0.5	7.2 $\pm$ 0.7	No immunotoxicity.
<b>RBC</b> ( $\times 10^6/\mu\text{L}$ )	7.2 $\pm$ 0.4	4.5-6.5	6.9 $\pm$ 0.3	7.1 $\pm$ 0.4	6.8 $\pm$ 0.5	Normal erythropoiesis
<b>Hemoglobin</b> (g/dL)	14.0 $\pm$ 1.0	13-17	13.5 $\pm$ 0.8	13.8 $\pm$ 0.9	13.2 $\pm$ 1.1	No anemia.
<b>Platelets</b> ( $\times 10^3/\mu\text{L}$ )	250 $\pm$ 20	150-450	240 $\pm$ 18	245 $\pm$ 15	235 $\pm$ 20	No clotting disruption.
<b>Lymphocytes</b> (%)	65 $\pm$ 5	20-40	68 $\pm$ 6	66 $\pm$ 5	70 $\pm$ 7	Possible immune stimulation or stress response

**Table 15: Presents Molecular Docking Results of *S. Typhi***

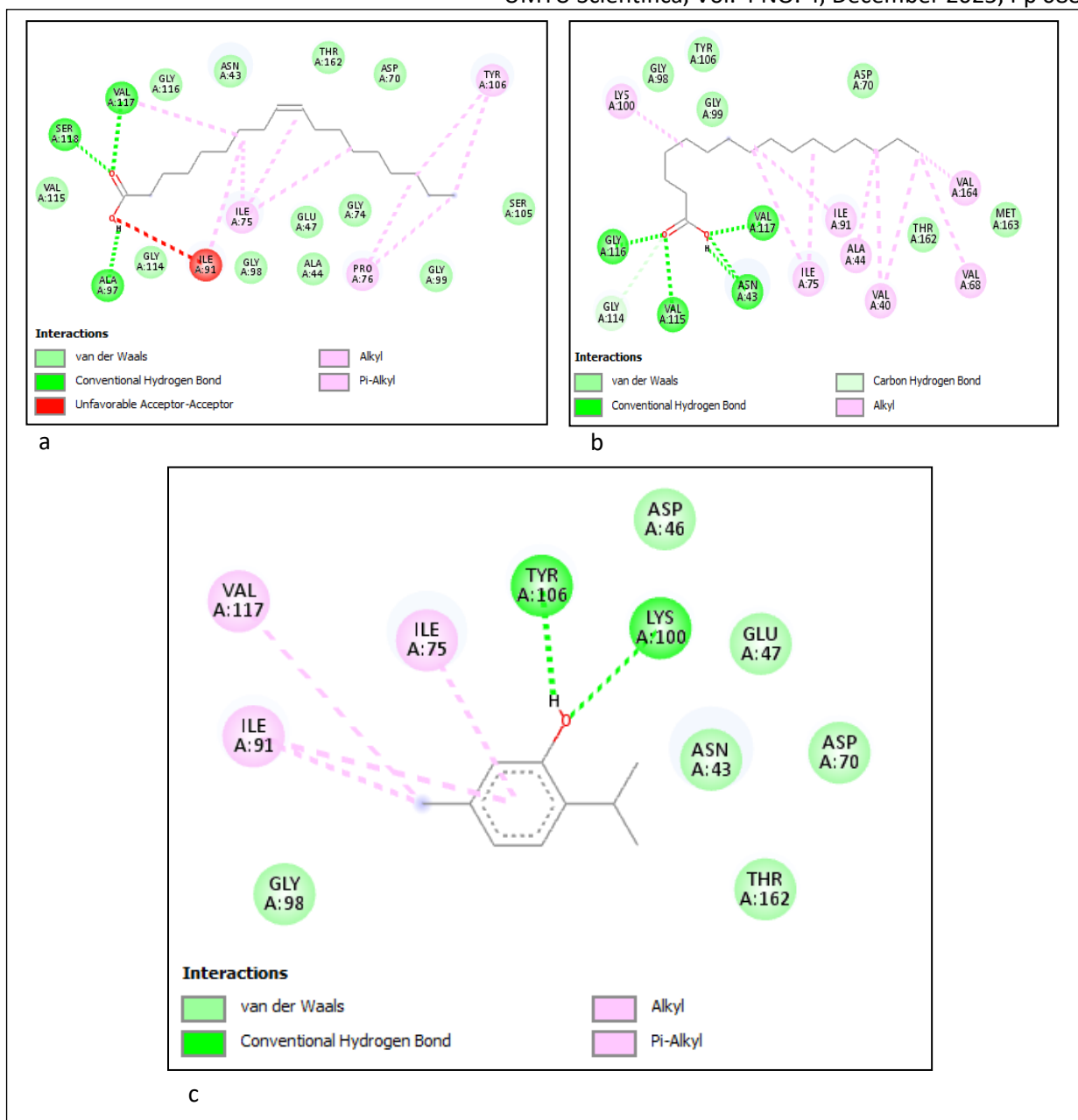
S/N	Phytocompound	DNA Gyrase	sipD
1	2-Phenylpropenal	-5.7	-5.3
2	Benzoic acid	-5.7	-5.2
3	Benzyl alcohol	-4.8	-4.7
4	Caryophyllene	-5.2	-6.1
5	Cis 11-Hexadecenal	-5.8	-5.3
6	DTBP	-5	-6.2
7	Elaidic acid	-5	-5.9
8	Limonene	-5.4	-5.5
9	Methyl-di- <i>t</i> -butylhydroxyhydrocinnamate	-5.7	-6.6
10	Methyl palmitate	-4.4	-4.5
11	Oleic acid	-6.4	-4.5
12	Palmitic acid	-5.8	-5.4
13	Thymol	-5.9	-5.6
<b>Reference Compounds</b>			
	Ciprofloxacin (Control Drug)	-8.5	-
	Native Ligand (sipD)	-	-7.1

## DISCUSSION

The study demonstrated the relevance of antimicrobial products and sought to evaluate the antimicrobial effects of medicinal plants used in the treatment of multidrug-resistant typhoid fever cases. The ethnopharmacology study will help codify the age-old experience of traditional healers in Katsina State into a rigorous, multifaceted scientific validation of plant-derived drugs for the treatment of multidrug-resistant typhoid fever (Olaniyi *et al.*, 2025).

Our results do not just reconfirm traditional use; they break down and highlight the intricate biochemical logic that underpins it, filled with cross-phytochemical interactions, multi-target mechanisms, and evolutionary gains, making these plants a powerful weapon in the fight

against antimicrobial resistance (Anand *et al.*, 2019). The study tested *Vernonia amygdalina* through its antimicrobial screening. It further establishes the link between ethnobotanical knowledge and laboratory science. The study shows the efficacy of *Vernonia amygdalina* on a isolates of clinical multidrug-resistant *Salmonella enterica* serovar *Typhi* isolates (Muazu *et al.*, 2024). The plant exhibits significantly pointed zones of inhibition and minimum inhibitory and bactericidal concentrations. This is not a random observation. Thus, it is the physicochemical manifestation of its varied phytochemicals. A similar effect was observed in clinical studies using leaf decoctions, with symptomatically improved individuals who were previously unresponsive to antibiotics (Muhammed *et al.*, 2021).



**Figure 15: Molecular interactions of *S. Typhi* DNA Gyrase B with identified phytochemicals (a) Oleic acid, (b) Palmitic acid and (c) Thymol**

By conducting phytochemical profiling using UHPLC-QTOF-MS and GC-MS, we found that *Vernonia amygdalina* has potential as a combinatorial therapy. It does not depend on a single silver-bullet compound but employs a coordinated synergy of bioactive agents, namely its characteristic bitter sesquiterpene lactones, as well as flavonoids and phenolic compounds, acting together (Okari *et al.*, 2024). Several studies have been conducted to investigate the antibacterial mechanisms of sesquiterpene lactones, vernodalin and vernolide, which are found in the active resinous exudate of the flowering Asteraceae plants. They act by weakening the cellular membrane, disrupting its integrity and protective barrier functions, allowing other antimicrobial elements access (Manayia *et al.*, 2025). At the same time, flavonoids such as quercetin and its derivatives act on bacterial cells to inhibit protein synthesis. These compounds bind to ribosomal subunits, altering the decoding of the genetic

code and disrupting bacterial growth and replication. Another part of this multi-pronged attack is to inhibit key bacterial enzymes, such as those in the shikimate pathway and fatty acid synthesis, to deprive it of metabolites necessary for its survival and replication. The simultaneous attack on multiple essential cellular processes, e.g., membrane integrity, protein synthesis, and core metabolism, would make it hard for the bacterium to develop resistance mutations that affect all mechanisms (Nguyen & Bhattacharya, 2022).

A significant and original finding of the research was the experimental confirmation of the strong synergy between *Vernonia amygdalina* and *Psidium guajava*. The combined extract acts in a more potent and distinct way than each component acting alone, not merely through additive effects but through synergistic effects (an emerging phenomenon). A study by Ekaluo *et al.* (2015) shows the pharmacological basis underlying this synergy and its

mechanistic basis. *Vernonia amygdalina* is the major attacking agent whose membrane-disrupting sesquiterpene lactones make pores that compromise the selective permeability of the bacterial cell membrane (Alara *et al.*, 2017). This breach does two important things. First, it causes the pathogen to die. Second, it opens a cavity that enhances the intracellular penetration and bioavailability of the bioactive flavonoids and tannins of

*Psidium guajava*. Once inside the cell at elevated concentrations, these constituents of *P. guajava* can more effectively target intracellular targets, such as DNA topoisomerases and essential virulence regulators (Kumar *et al.*, 2021). Furthermore, components within *P. guajava* appear to act as efflux pump inhibitors, i.e., they inhibit the bacterium's primary mechanism for expelling toxic compounds.

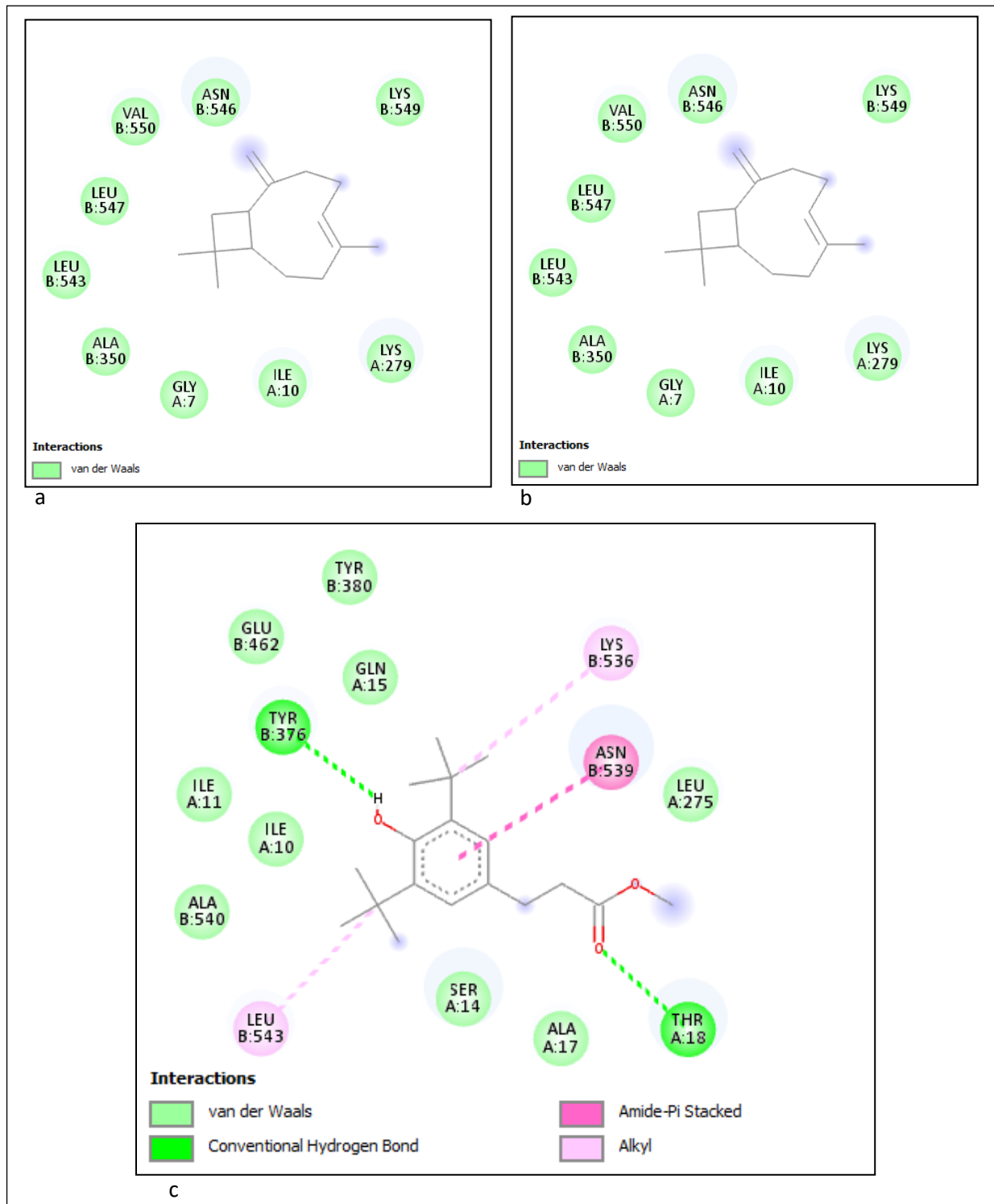


Figure 16: Molecular interactions of *S. Typhi* SipD with identified phytochemicals (a) Carryophyllene, (b) DTBP and (c) Methyl di-t-butyl hydroxyhydrocinnamate

This, in turn, keeps the phytochemicals trapped inside the cell, resulting in constant exposure to a lethal concentration. This powerful partnership disrupts

virulence; the concoction displays a significant ability to interfere with the Type III Secretion System (T3SS) – a needle-like syringe used by *S. Typhi* to inject effector

proteins into host cells, which can neutralize its capacity to invade and survive intracellularly. The combination of four synergistic mechanisms of action, such as membrane disruption, improved bioavailability, efflux-pump inhibition, and virulence attenuation, represents a robust herbal therapeutic design for the development of resistance-resistant combination therapies. As a result, this approach can serve as a model for designing a variety of new herbal alternatives (Huynh *et al.* 2025).

In silico docking studies offer an atomic-level view of these interactions, providing predictive models of the relationship between bioactivity and the molecular mechanism. The study found that several important phytochemicals, including oleic acid and various terpenoids identified in the GC-MS analysis, have very high and specific binding affinities for important bacterial protein targets. For example, the predicted binding of oleic acid to the DNA gyrase binding site suggests a competitive inhibition mechanism, leading to the displacement of cofactors required for the enzyme to perform its functions in DNA replication and transcription. This interaction is predicted to occur outside the quinolone-binding site, potentially conferring effectiveness against fluoroquinolone-resistant strains with *gyrA* mutations. Likewise, analysis of docking of substances such as methyl di-*t*-butyl hydroxyhydrocinnamate to the SipD protein of the virulence-associated T3SS suggest a virulence-inhibiting mechanism by which the phytochemical physically occludes the translocation pore or induces conformational changes that prevent proper assembly and function of this invasion system. According to the computational results, it is easy to understand the antibacterial and anti-virulence properties obtained from the in vitro experiments, and it provides a structural blueprint for future semi-synthetic modification to enhance potency and pharmacokinetic properties (Hazra *et al.*, 2023).

For any therapeutic agent to be transitioned from customary to clinical use, a clear understanding of the safety profile is of great importance, and our extensive toxicological evaluation provides ample, reassuring data in this regard. Both single extracts and the synthesis of various (different) types of extracts are classified as standards and/or mixtures of these extracts and have 30% fat acceptable. When we used doses much higher than needed for the medicine to work, nothing bad happened. We did not observe the death of any experimental animals, nor did we observe any other adverse effects. A detailed evaluation of the liver, kidney, and other organs showed only slight, adaptive changes at the highest doses, with no necrosis, fibrosis or other evidence of irreversible organ damage. The serum markers for hepatic and renal function, assessed biochemically, confirmed this, with only temporary changes and full reversibility after stopping the treatment. This convincing toxicology file demonstrates a wide therapeutic index, supported by scientific studies, and supports the further development of these plants. It is in line with their long history of safety in traditional medicine and alleviates one of the major

concerns associated with herbal therapeutics (Dandashire *et al.* 2019).

## CONCLUSION

*Vernonia amygdalina* and *Psidium guajava* and show potential in treating typhoid fever, especially multidrug-resistant *S. Typhi*. The bioactive compounds present in these plants exhibit strong antimicrobial activity through multiple mechanisms. The most notable of these are bacterial membrane disruption, enzyme inhibition, and disruption of virulence factors. The benefits of the synergistic effects of plant extracts suggest that better therapeutic efficacy could be achieved with polyherbal formulations, which could help impede the development of resistance. These extracts are not toxic to living systems at biologically active concentrations and may be useful in further drug development. This study connects the traditional use of natural compounds for healing with modern technology to develop affordable alternatives. This can tackle resistant infections in countries where medicines may not be affordable. To improve the management of typhoid and other microbes, the therapeutic efficacy, safety, mechanisms of action, standardisation, and clinical applicability of plants and their active principles should be validated in future research.

## REFERENCES

- Agu, P. C., Afiukwa, C. A., Orji, O. U., Ezech, E. M., Ofoke, I. H., Ogbu, C. O., Ugwuja, E. I., & Aja, P. M. (2023). Molecular docking as a tool for the discovery of molecular targets of nutraceuticals in diseases management. *Scientific Reports*, *13*, 13398. [Crossref]
- Åhman, J., Matuschek, E., & Kahlmeter, G. (2022). Evaluation of 10 brands of pre-poured Mueller-Hinton agar plates for EUCAST disc diffusion testing. *Clinical Microbiology and Infection*, *28*(4), 610–614. [Crossref]
- Ahmed, S., Hassan, M. R., Yakubu, L. L., Ajala, M. K., Rekwot, G. Z., & Abdulmumini, L. (2025). Assessment of livelihood strategies adopted among camels herders in north-west, Nigeria. *Journal of Agricultural and Pastoral Studies*, *1*(2), 121–128. [Crossref]
- Ajegi, I. F., Ajegi, G. O., Ajaegbu, O. C., Nwokike, M. O., Ramalan, M. A., Eje, V. I., & Akuodor, G. C. (2023). Evaluation of the antiulcer and antimicrobial activities of methanol leaf extract of *Helianthus annuus*. *International Journal of Basic & Clinical Pharmacology*, *12*(2), 161–167. [Crossref]
- Alara, O. R., Abdurahman, N. H., Abdul Mudalip, S. K., & Olalere, O. A. (2017). Phytochemical and pharmacological properties of *Vernonia amygdalina*: A review. *Journal of Chemical Engineering and Industrial Biotechnology*, *2*(1), 80–96. [Crossref]
- Al-Khafaji, N. S. K., Al-Bayati, A. M. K., & Al-Dahmoshi, H. O. M. (2021). Antimicrobial resistance in *Salmonella Typhi*. In *Current Topics in Bacterial Infections* (pp. 45–60). IntechOpen. [Crossref]

- Amusa, M. O., Cuboia, N., & Olofinsan, K. (2024). Medicinal plants used in the treatment of typhoid fever in Nigeria: A systematic review. *Journal of Herbal Medicine*, 47, 100930. [Crossref]
- Anand, U., Jacobo-Herrera, N., Altemimi, A., & Lakhssassi, N. (2019). A comprehensive review on medicinal plants as antimicrobial therapeutics: Potential avenues of biocompatible drug discovery. *Metabolites*, 9(11), 258. [Crossref]
- Bhandari, J., Thada, P. K., Hashmi, M. F., & DeVos, E. (2024, April 19). Typhoid fever. In *StatPearls*. StatPearls Publishing. [Link]
- Bin Eric, M., Netongo, P. M., Kamdem, S. D., Nzuno, C., Tchoutang, A. M., Berenger, T. K. E., Ateba, F. O., & Mbacham, W. F. (2025). Stress-mediating inflammatory cytokine profiling reveals unique patterns in malaria and typhoid fever patients. *PLOS ONE*, 20(2), e0306585. [Crossref]
- Brown, S. T., Mohammed, I. U., & Umaru, I. J. (2024). Antimicrobial activity of paw-paw (*Carica papaya*) leaves and seed extracts on *Shigella* and *Salmonella* species. *African Journal of Clinical Medicine and Pharmacy Research*, 1(1). [Crossref]
- Centers for Disease Control and Prevention. (2023). *CDC yellow book 2024: Health information for international travel*. Oxford University Press.
- Chan, E. Y. Y., Tong, K. H. Y., Dubois, C., Mc Donnell, K., Kim, J. H., Hung, K. K. C., & Kwok, K. O. (2021). Narrative review of primary preventive interventions against water-borne diseases: Scientific evidence of health-EDRM in contexts with inadequate safe drinking water. *International Journal of Environmental Research and Public Health*, 18(23), 12268. [Crossref]
- Chen, C.-Y., Li, Y.-H., Li, Z., & Lee, M.-R. (2023). Characterization of effective phytochemicals in traditional Chinese medicine by mass spectrometry. *Mass Spectrometry Reviews*, 42(5), 1808–1827. [Crossref]
- Chen, X. F., Ding, Y. Y., Guan, H. R., Zhou, C. J., He, X., Shao, Y. T., & Chen, S. H. (2024). The pharmacological effects and potential applications of limonene from Citrus plants: A review. *Natural Product Communications*, 19(5). [Crossref]
- Clinical and Laboratory Standards Institute. (2023). *Performance standards for antimicrobial susceptibility testing* (33rd ed.). CLSI supplement M100.
- Dandashire, B. S., Magashi, A. M., Abdulkadir, B., Abbas, M. A., Goni, M. D., & Yakubu, A. (2019). Toxicological studies and bioactivity-guided identification of antimicrobially active compounds from crude aqueous stem bark extract of *Boswellia dalzielii*. *Journal of Advanced Veterinary and Animal Research*, 6(2), 183–192. [Crossref]
- de Melo, L. F. M., Aquino-Martins, V. G. de Q., da Silva, A. P., Rocha, H. A. O., & Scortecchi, K. C. (2023). Biological and pharmacological aspects of tannins and potential biotechnological applications. *Food Chemistry*, 423, 135645. [Crossref]
- Devi, P. (2022). *Paper strip based assay for the detection of Salmonella* [Doctoral dissertation, National Dairy Research Institute]. Krishikosh. [Link]
- Dubale, S., Kebebe, D., Zeynudin, A., Abdissa, N., & Suleman, S. (2023). Phytochemical screening and antimicrobial activity evaluation of selected medicinal plants in Ethiopia. *Journal of Experimental Pharmacology*, 15, 51–62. [Crossref]
- Ekaluo, U. B., Ikpeme, E. V., Ekerette, E., & Chukwu, C. I. (2015). In vitro antioxidant and free radical activity of some Nigerian medicinal plants: Bitter leaf (*Vernonia amygdalina* L.) and guava (*Psidium guajava* Del.). *Research Journal of Medicinal Plant*, 9(5), 215–226. [Crossref]
- Enders, A. A., North, N. M., Fensore, C. M., Velez-Alvarez, J., & Allen, H. C. (2021). Functional group identification for FTIR spectra using image-based machine learning models. *Analytical Chemistry*, 93(28), 9711–9718. [Crossref]
- Ge, J., Li, X., Lu, Q., Li, S., Liu, J., Deng, X., Wang, Y., & Qiu, J. (2025). Isopropyl paraben targets type III secretion to inhibit *Salmonella enterica* serovar Typhimurium infection. *Virulence*, 16(1), 2548621. [Crossref]
- Greene, A. M., Teixidor-Toneu, I., & Odone, G. (2023). To pick or not to pick: Photographic voucher specimens as an alternative method to botanical collecting in ethnobotany. *Journal of Ethnobiology*, 43(1), 44–56. [Crossref]
- Han, X., Zhang, A., Meng, Z., Wang, Q., Liu, S., Wang, Y., Tan, J., Guo, L., & Li, F. (2024, September 30). Bioinformatics analysis based on extracted ingredients combined with network pharmacology, molecular docking and molecular dynamics simulation to explore the mechanism of Jinbei oral liquid in the therapy of idiopathic pulmonary fibrosis. *Helvion*, 10(18), e38173. [Crossref]
- Hazra, S., Ray, A. S., Das, S., Das Gupta, A., & Rahaman, C. H. (2023). Phytochemical profiling, biological activities, and in silico molecular docking studies of *Causonis trifolia* (L.) Mabb. & J.Wen shoot. *Plants*, 12(7), 1495. [Crossref]
- Huynh, H. D., Nargotra, P., Wang, H. M. D., Shieh, C. J., Liu, Y. C., & Kuo, C. H. (2025). Bioactive compounds from guava leaves (*Psidium guajava* L.): Characterization, biological activity, synergistic effects, and technological applications. *Molecules*, 30(6), 1278. [Crossref]
- Krakowska-Sieprawska, A., Kielbasa, A., Rafińska, K., Ligor, M., & Buszewski, B. (2022). Modern methods of pre-treatment of plant material for the extraction of bioactive compounds. *Molecules*, 27(3), 730. [Crossref]
- Kumar, M., Tomar, M., Amarowicz, R., Saurabh, V., Nair, M. S., Maheshwari, C., Sasi, M., Prajapati, U., Hasan, M., Singh, S., Changan, S., Prajapat, R. K., Berwal, M. K., & Satankar, V. (2021). Guava (*Psidium guajava* L.) leaves: Nutritional composition, phytochemical profile, and health-promoting bioactivities. *Foods*, 10(4), 752. [Crossref]

- Manaya, A. H., Ilhami, F., & Puspitarini, S. (2025). Investigation of phytochemicals and antibacterial efficacy in flower extracts of *Vernonia amygdalina*: Complemented molecular docking analysis. *Journal of the Indian Chemical Society*, 101, 101604. [\[Crossref\]](#)
- Muazu, A., Usman, A., & Usman, H. D. (2024). Antibacterial activity of *Vernonia amygdalina* (bitter leaf) extracts against clinical isolates of *Salmonella* species. *UMYU Journal of Microbiology Research (UJMR)*, 2(4), 37–43.
- Muhammed, D., Ado, A., & Adamu, H. (2024). Phytochemical screening and antimicrobial activity of *Vernonia amygdalina* against some clinical isolates. *Nigerian Journal of Animal Production*, 405–410. [\[Crossref\]](#)
- Nguyen, T. L. A., & Bhattacharya, D. (2022). Antimicrobial activity of quercetin: An approach to its mechanistic principle. *Molecules*, 27(8), 2494. [\[Crossref\]](#)
- Okari, K. A., Ezekwe, A. S., & Wokocha, P. G. (2024). Phytochemical profile and bioactive compounds in aqueous leaf extract of *Vernonia amygdalina* (Asteraceae): A GC-MS analysis. *Asian Journal of Research in Biochemistry*, 14(6), 117–123. [\[Crossref\]](#)
- Olaniyi, T. D., Adetutu, A., & Amusa, M. O. (2025). Typhoid fever and medicinal plants review: A case study in Nigeria. *KIU Journal of Health Sciences*, 4(2), 22–48. [\[Crossref\]](#)
- Rigby, S. P. (2024). Uses of molecular docking simulations in elucidating synergistic, additive, and/or multi-target (SAM) effects of herbal medicines. *Molecules*, 29(22), 5406. [\[Crossref\]](#)
- Sankar, K., Billah, M. A., Selvarajan, S., Madhumitha, N., Rangarajan, S., Monisha, R. L., & Madesh, L. (2025). A comprehensive assessment of the antimicrobial resistance and antibiogram profiles in healthcare settings among the Indian population [Conference abstract]. In M. Simões & M. Maresca (Eds.), Abstracts of the 4th International Electronic Conference on Antibiotics. *Medical Sciences Forum*, 35(1), 1. [\[Crossref\]](#)
- Shaikh, N., Swali, P., & Houben, R. M. G. J. (2023). Asymptomatic but infectious: The silent driver of pathogen transmission. A pragmatic review. *Epidemics*, 44, 100704. Advance online publication. [\[Crossref\]](#)
- Shaikh, O. A., Asghar, Z., Aftab, R. M., Amin, S., Shaikh, G., & Nashwan, A. J. (2023). Antimicrobial resistant strains of *Salmonella typhi*: The role of illicit antibiotics sales, misuse, and self-medication practices in Pakistan. *Journal of Infection and Public Health*, 16(11), 1717–1723. [\[Crossref\]](#)
- Sisay, W., Engidawork, E., & Shibeshi, W. (2021). Evaluation of the antidiarrheal activity of the hydromethanolic extract of the leaves of *Rumex nepalensis* in mice. *BMC Complementary Medicine and Therapies*, 21, 150. [\[Crossref\]](#)
- Sosa, A. A. (2025). Secondary metabolites profiling using FTIR and GC-MS techniques and bioactivities of fennel (*Foeniculum vulgare*) aerial parts and evaluation of its antioxidant (singlet oxygen scavenging and hypochlorous acid scavenging) activity. *South Asian Research Journal of Agriculture and Fisheries*, 7(2), 25–33. [\[Crossref\]](#)
- Sundaram, R. L., Raju, S., & Oruganti, S. (2021). Acute and sub-acute oral toxicity assessment of *Gracilaria edulis* in Sprague-Dawley rats. *Toxicology Reports*, 8, 1601–1611. [\[Crossref\]](#)
- Truong, D. H., Nguyen, D. H., Ta, N. T. A., Bui, A. V., Do, T. H., & Nguyen, H. C. (2019). Evaluation of the use of different solvents for phytochemical constituents, antioxidants, and in vitro anti-inflammatory activities of *Severinia buxifolia*. *Journal of Food Quality*, 2019, 8178294. [\[Crossref\]](#)
- Truong, W. R., Hidayat, L., Bolaris, M. A., Nguyen, L., & Yamaki, J. (2021). The antibiogram: key considerations for its development and utilization. *JAC-Antimicrobial Resistance*, 3(2), dlab060. [\[Crossref\]](#)
- Verep, D., Ateş, S., & Karaoğul, E. (2023). A review of extraction methods for obtaining bioactive compounds in plant-based raw materials. *Bartın Orman Fakültesi Dergisi Journal of Bartın Faculty of Forestry*, 25(3), 492–513. [\[Crossref\]](#)
- Wallie, M. B., Amenyah, S. D., & Guenne, S. (2021). Phytochemical screening and GC-MS analysis of the bioactive compounds in the bark extract of *Zanthoxylum gillettii*. *Journal of Phytopharmacology*, 10(6), 453–458. [\[Crossref\]](#)
- Willie, P., Uyoh, E. A., & Aikpokpodion, P. O. (2021). Gas chromatography-mass spectrometry (GC-MS) assay of bio-active compounds and phytochemical analyses in three species of apocynaceae. *Pharmacognosy Journal*, 13(2), 524–537. [\[Crossref\]](#)
- World Health Organization. (2023, March 30). *Typhoid*. Retrieved October 30, 2024, from [\[Link\]](#)
- Xu, L., Yang, J., Zhang, Y., Liu, X., Liu, Z., Sun, F., Ma, Y., Wang, L., & Xing, F. (2024). Mining of gene modules and identification of key genes for early diagnosis of gastric cancer. *International Journal of Pharmaceutical Research and Allied Sciences*, 13(1), 26–38. [\[Crossref\]](#)
- Zafar, M. A., Hernandez, G. E., & Walker, K. A. (2024). Mechanisms of bacterial host-to-host transmission. *Microbiology and Molecular Biology Reviews*, 88(4), e00259-24. [\[Crossref\]](#)
- Zhang, L. F., Lepenies, B., Nakamae, S., Young, B. M., Santos, R. L., Raffatellu, M., Cobb, B. A., Hiyoshi, H., & Bäumlner, A. J. (2022). The Vi capsular polysaccharide of *Salmonella Typhi* promotes macrophage phagocytosis by binding the human C-type lectin DC-SIGN. *mBio*, 13(6), e02733-22. [\[Crossref\]](#)
- Zhang, W., Gao, L., Wang, C., Wang, S., Sun, D., Li, X., Liu, M., Qi, Y., Liu, J., & Lin, B. (2020). Combining bioinformatics and experiments to identify and verify key genes with prognostic values in endometrial carcinoma. *Journal of Cancer*, 11(3), 716–732. [\[Crossref\]](#)